THE ANATOMICAL RECORD 263:167–185 (2001)

Modeling and Remodeling in a Developing Artiodactyl Calcaneus: A Model for Evaluating Frost's Mechanostat Hypothesis and Its Corollaries

JOHN G. SKEDROS, MARK W. MASON, AND ROY D. BLOEBAUM*
Bone and Joint Research Laboratories, Department of Veterans Affairs SLC Health Care System, Salt Lake City, Utah

ABSTRACT

The artiodactyl (mule deer) calcaneus was examined for structural and material features that represent regional differences in cortical bone modeling and remodeling activities. Cortical thickness, resorption and formation surfaces, mineral content (percent ash), and microstructure were quantified between and within skeletally immature and mature bones. These features were examined to see if they are consistent with predictions of Frost's Mechanostat paradigm of mechanically induced bone adaptation in a maturing "tension/compression" bone (Frost, 1990a,b, Anat Rec 226:403–413, 414–422). Consistent with Frost's hypothesis that surface modeling activities differ between the "compression" (cranial) and "tension" (caudal) cortices, the elliptical cross-section of the calcaneal diaphysis becomes more elongated in the direction of bending as a result of preferential (> 95%) increase in thickness of the compression cortex. Regional differences in mineral content and population densities of new remodeling events (NREs = resorption spaces plus newly forming secondary osteons) support Frost's hypothesis that intracortical remodeling activities differ between the opposing cortices: 1.) in immature and mature bones, the compression cortex had attained a level of mineralization averaging 8.9 and 6.8% greater ($P < 0.001$), respectively, than that of the tension cortex, and 2.) there are on average 350 to 400% greater population densities of NREs in the tension cortices of both age groups ($P < 0.0003$). No significant differences in cortical thickness, mineral content, porosity, or NREs were found between medial and lateral cortices of the skeletally mature bones, suggesting that no modeling or remodeling differences exist along a theoretical neutral axis. However, in mature bones these cortices differed considerably in secondary osteon cross-sectional area and population density. Consistent with Frost's hypothesis, remodeling in the compression cortex produced bone with microstructural organization that differs from the tension cortex. However, the increased remodeling activity of the tension cortex does not appear to be related to a postulated low-strain environment. Although most findings are consistent with *predictions* of Frost's Mechanostat paradigm, there are several notable inconsistencies. Additional studies are needed to elucidate the nature of the *mechanisms* that govern the modeling and remodeling activities that produce and maintain normal bone. It is proposed that the artiodactyl calcaneus will provide a useful experimental model for these studies. Anat Rec 263:167–185, 2001.

Key words: bone adaptation; mechanostat theory; bone mineral content; mule deer; osteons

Grant sponsor: Department of Veterans Affairs.

*Correspondence to: Roy D. Bloebaum, Ph.D., Bone and Joint Research Laboratories (151F), Department of Veterans Affairs SLC Health Care System, 500 Foothill Blvd., Salt Lake City, UT 84148. E-mail: roy.bloebaum@hsc.utah.edu

Received 16 November 1999; Accepted 1 March 2001

In recent studies, the artiodactyl (e.g., sheep and deer) calcaneus has been described as a simply loaded "tension/compression" bone (Skedros and Bloebaum, 1991; Skedros et al., 1993c, 1994a,b, 1997). In vivo and in vitro data demonstrate that, during physiologic weight-bearing activities, the calcaneal diaphysis behaves similar to a cantilevered beam with longitudinal compression and tension strains[1] predominating on opposite cranial and caudal cortices, respectively (Lanyon, 1974; Su et al., 1999). Skedros and coworkers (1994a,b, 1997) documented significant regional differences in cortical thickness, mineral content (% ash), and microstructure (e.g., secondary osteon population densities and osteon morphology) in skeletally mature calcanei. They speculated that these unusually conspicuous structural and material heterogeneities represent the outcome of adaptive bone modeling and remodeling responses to a long history of the functional cranial-caudal compression-tension strain distribution. They also recognized that these apparent structural and material adaptations were consistent with *predictions* of Frost's Mechanostat paradigm (i.e., the Mechanostat hypothesis and its corollaries) for mechanically induced bone adaptations in the specific case of a "tension/compression" bone (Table 1) (Frost, 1983, 1987, 1988a,b, 1990a,b). The Mechanostat paradigm is based largely on the idea that mechanically induced bone strains are important in governing *threshold*-related activation and control of bone modeling and remodeling processes (see Appendix). Although not rigorously tested in controlled experimental studies, this paradigm is commonly used in current basic and clinical literature as a modern version of Wolff's law of mechanically mediated bone adaptation. Recognizing that predictions of modeling and remodeling activities in a developing bone have been largely based on unquantified observations, indirect inferences, and anecdotal clinical cases (Frost, 1988a, 1990a,b), Frost has called for quantitative investigations that are designed to examine the validity of the modeling and remodeling rules of the Mechanostat paradigm (Frost, 1983, 1987, 1988a,b, 1990a,b).

Because Skedros et al. (1994a,b, 1997) examined only skeletally mature bones, they could not evaluate ontogenetic changes in the modeling and remodeling responses in this context. The goal of the present study was to determine if a selected set of *predictions* of the Mechanostat paradigm can be supported through quantitative analysis of skeletally immature and mature artiodactyl calcanei. We hypothesize that this analysis will demonstrate the specific tension- and compression-related regional variations listed in Table 1. Additionally, in the context of this analysis, studies that have produced data that support or challenge the Mechanostat paradigm are briefly summarized. In view of results of the present investigation and contradictory findings among some of these previous studies, it is also suggested that the artiodactyl calcaneus will be a useful experimental model for clarifying the role of Frost's Mechanostat paradigm in predicting bone development, maintenance, and adaptation.

TABLE 1. Frost's predicted outcomes of maturation-related modeling and remodeling in the diaphysis of a "tension/compression" bone*

Structure/architecture (regional cortical thickness differences and cross-sectional shape)
Increase in long axis of elliptical cross section in direction of bending
Cortical drift by bone apposition primarily on the compression cortex
Resorption along the endosteal surface of the cranial cortex[a]
Equivalent cortical thickness in the medial and lateral cortices (i.e., along a neutral axis)
Material/tissue-entire cortex
Compression cortex vs. tension cortex
Increased mineralization in the compression cortex
Smaller BMUs (secondary osteons)[b] in the compression cortex
Decreased porosity in the compression cortex
Medial cortex vs. lateral cortex (i.e., opposing cortices along a neutral axis)
Equivalent mineralization in medial and lateral cortices
Equivalent microstructure and porosity in medial and lateral cortices[a]
Compression or tension cortex vs. medial and lateral cortices
Increased porosity and remodeling activity in the tension cortex[c]
Cortical regions-"tension/compression" cortices (periosteal vs. middle vs. endosteal)
Larger BMUs (secondary osteons) in the endosteal regions
Increased porosity in the endosteal regions

*Adapted from Frost (1988a,b, 1990a,b).
[a]The data reported in the present study are not consistent with these predictions.
[b]BMU = basic multicellular unit, which is a forming secondary osteon. Frost considers a fully formed secondary osteon as a basic structural unit (BSU). In the present study, no distinction is made between BMUs and BSUs; they are both considered as secondary osteons that are either fully formed or in some state of formation.
[c]Conventional predictions would also include increased remodeling (increased porosity and decreased mineral content) in "neutral axis" (medial and lateral) regions. The predictions listed above, however, reflect knowledge that such regions receive significant shear strains and principal strains that are oblique to the long axis of the bone (i.e., "oblique" in the sense that they are oriented in a direction that significantly deviates from the longitudinal diaphyseal axis). (Compare Frost (2000a) and Turner (2000) for further discussion about shear strains at the neutral axis.)

MATERIALS AND METHODS

Model

The diaphyseal region of the mule deer calcaneus (Fig. 1) was selected as the representative model because it is the most beam-like of common artiodactyl calcanei (Schmid, 1972). Su et al. (1998, 1999) performed rigorous in vitro strain analyses on mule deer calcanei using 7 rosette strain gauges on each bone. Their study showed

[1]In its simplest definition, mechanical strain is the change in length of a loaded structure as a percentage of its initial (unloaded) length. This unit-less ratio is a measure of material or tissue deformation. In vivo strain data on a variety of animals suggests that physiologically normal strains are between 200 and 2,500 microstrain (i.e., between 0.02 and 0.25% change in length) in compression (Biewener et al., 1983a,b, 1986; Rubin and Lanyon, 1985). The upper limit may be only 1,500 microstrain in tension. Stress and strain are related by Hooke's law, which says that they are proportional to one another. Available data favor strain, instead of stress, as the mechanical parameter involved in mediating bone adaptations (Lanyon, 1987; Rubin and Lanyon, 1984).

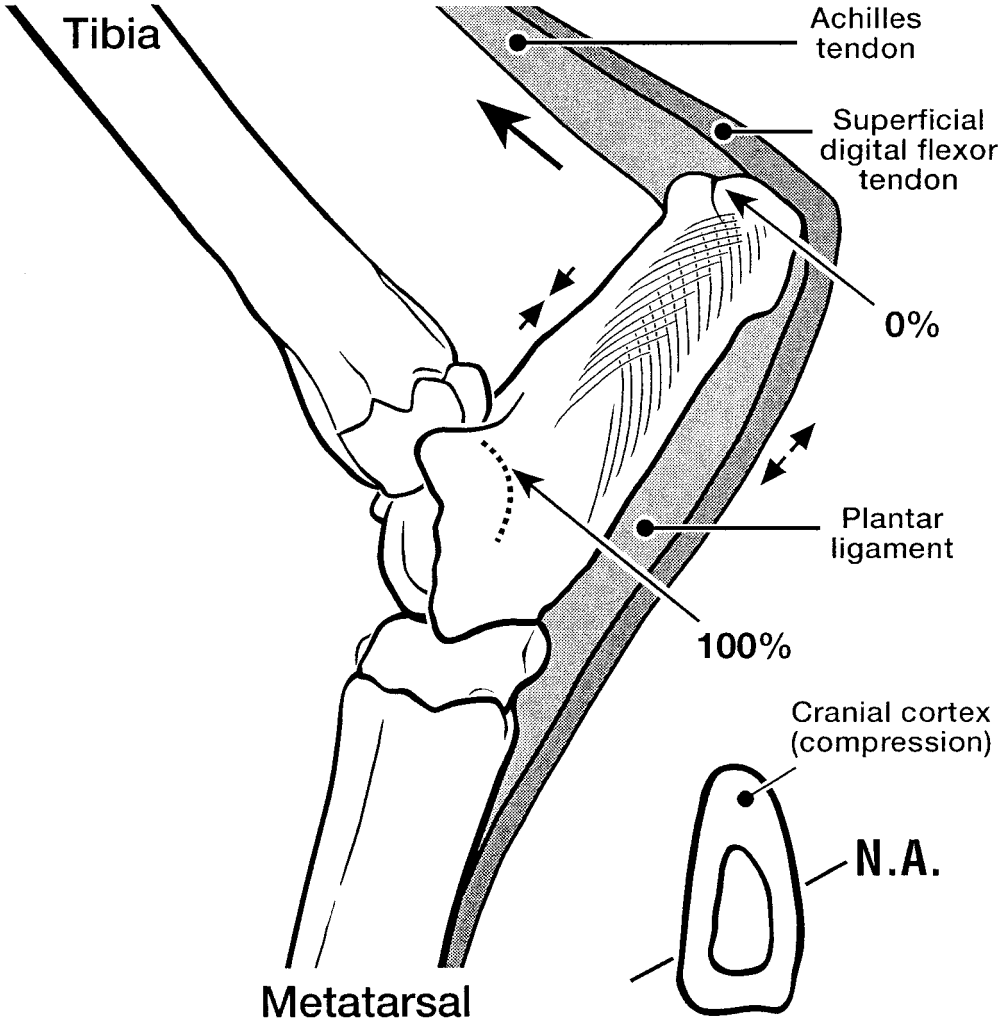

Fig. 1. Lateral-to-medial view of the ankle region of a skeletally mature mule deer showing the calcaneus shaft "length: and other associated bones, ligaments, and tendons. The trabecular patterns are stylized, and are based on a lateral-to-medial roentgenogram. Comparison of this drawing to Frost's idealized "tension/compression" bone in Figure 2 shows that the artiodactyl calcaneus differs in several ways: 1.) its shaft is relatively straight, 2.) it is cantilevered, 3.) the plantar ligament forms a firmly adherent "tension member" along its caudal cortex, and 4.) cancellous bone completely fills the medullary canal along approximately 60% of its shaft length. The dotted line at the tip of the 100% arrow indicates the projected location of the contour formed by the talus-calcaneus articular surfaces. The large cranial-directed arrow indicates the direction of force imparted by the Achilles tendon during mid-stance, loading the cranial cortex in compression (Su et al., 1999). The cross-section is from the 60% location and shows the relatively thicker cranial cortex. An approximate location of the "neutral" axis (NA) is also shown (estimated from measurements of Su, 1998; Su et al., 1999).

that functional loading of the diaphyseal region produces a strain milieu similar to that of an idealized nonprismatic cantilevered beam and approximates the strain distribution in the idealized "tension/compression" bone described by Frost (1990a,b) (Fig. 2). During simulated midstance phase of various gaits, the cranial calcaneus exhibits peak compressive strains on the order of 350 to 1,100 microstrain ($\mu\epsilon$) (491 to 1962N end load, respectively) and the caudal calcaneus exhibits estimated peak tensile strains on the order of 380 to 940 $\mu\epsilon$ (491 to 1962N end load, respectively) (491N and 1962N correspond to approximately 0.3 and 1.0 times body weight, respectively). At these loads, strains on the medial and lateral cortices were also notable (medial: 390 to 1,330 $\mu\epsilon$ in compression; lateral: 350 to 1,170 $\mu\epsilon$ in tension) even though these regions are considered to be on a neutral axis where longitudinal strains are minimal. These results reflect the fact that the peak strains along these medial and lateral locations are significantly *oblique* to the bone's longitudinal axis. Su et al. (1999) also showed that caudal cortex strains were tensile even with an intact plantar ligament. The customary tension-compression strain milieu of the mule deer calcaneus also resembles in vivo strain milieus on sheep and potoroo (a small marsupial) calcanei (Biewener et al., 1996; Lanyon, 1974; Su et al., 1999).

Specimens

Two calcanei were obtained from each of 34 male Rocky Mountain mule deer (Odocoileus hemionus hemionus) that had been taken to a game processing facility (Davis County, UT) during late October of a Fall hunting season. At the time of specimen collection, the periosteal ("velvet")

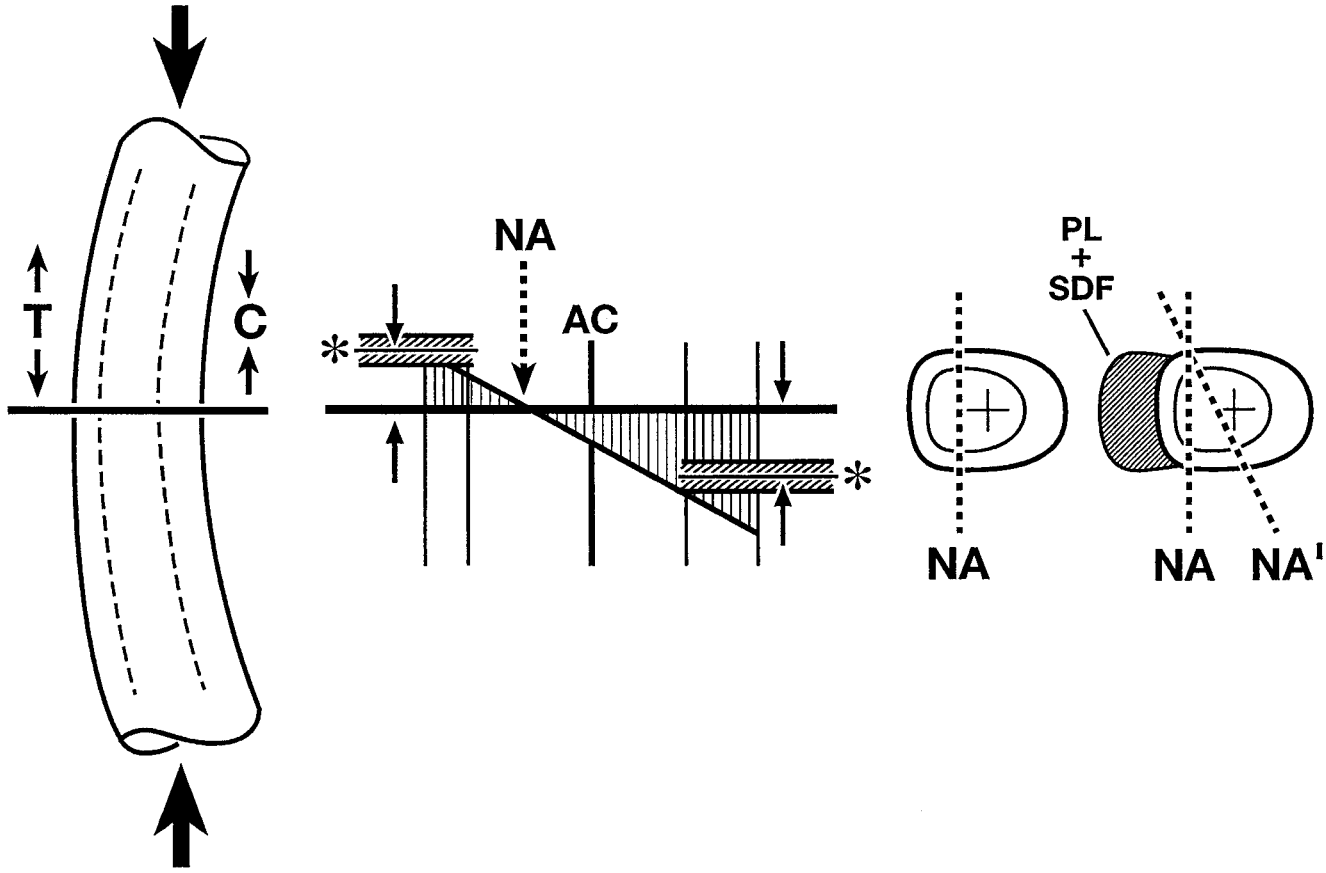

Fig. 2. This figure illustrates how the strain magnitudes govern *remodeling* activities in accordance with the Mechanostat hypothesis. **Left:** The combined loading (axial compression and bending) of Frost's idealized diaphyseal segment of a limb bone. **Center:** The strain distribution across the horizontal line of the bone segment. Shown are the anatomic center (AC) of the bone, neutral axis (NA), average minimum effective strain of remodeling (MESr) values (asterisks and paired vertical arrows), and MESr ranges (narrow paired parallel horizontal lines with intervening oblique lines). Note that the customary strains (vertical lines) on the tension side (left side of drawing) of the strain distribution fall below the average MESr across the entire breadth of the cortex. In contrast, the customary strains (vertical lines) across the entire breadth of the compression cortex typically exceed the average MESr. Accordingly, if the entire tension cortex exists in a state of perceived disuse, then it would exhibit active osteonal remodeling (see Fig. 8). In contrast, the entire breadth of the compression cortex would have very little remodeling activity since its strain milieu is within the interval between its MESr and the threshold for high-strain or microdamage-mediated remodeling. The cross-sections show that during over-loading, the NA shifts towards the tension cortex, reducing strain magnitudes. **Right:** When the functional contributions of the tension-carrying plantar ligament (PL) and tendon of the superficial digital flexor (SDF) of the deer calcaneus are considered, peak caudal strains are further reduced because the NA shifts even farther toward the caudal cortical surface. This illustrates the important mechanical role that associated fibroelastic tissues have in altering customary strain distributions and magnitudes during functional end-loading of the calcaneal shaft (Su et al., 1999). NA' represents the customary oblique orientation of the neutral axis shown in the in vitro functional loading study of Su et al. (1999). Reproduced, with revision, from Frost (1990b) with permission of the publisher.

covering of the antlers had been shed and antler growth was complete. Studies by Banks et al. (1968) and Hilmann et al. (1973) have shown that the relatively minor amount of appendicular cortical bone that had been resorbed for the demands of antler growth would have been replenished. Since the hunt was 2 to 4 weeks before the mating season, the animals had not yet participated in aggressive physical interactions characteristic of the rut (Anderson, 1981; Goss, 1983). These facts diminish the possibility that current remodeling activities are the result of metabolic demands of antler growth and/or repair of bone microdamage caused during the rut. Using the presence or absence of cartilage at the distal growth plate near the insertion of the Achilles tendon (Purdue, 1983), the paired calcanei were separated into skeletally mature (n = 15) and immature (n = 19) groups. Although we could not locate information regarding animal age and epiphyseal closure in limb bones of male Rocky Mountain mule deer, comparative data are available in the black-tailed deer subspecies (Odocoileus hemionus columbianus). Lewall and Cowan (1963) and Purdue (1983) reported that the epiphyseal plates at the free (distal) end of calcanei of white- and black-tailed deer are half-fused by approximately 20–26 months postpartum. Extrapolating these data allows a conservative estimate that epiphyseal closure in the calcaneus of the closely related Rocky Mountain mule deer occurs between 2 and 3 years of age, which is consistent with an estimated age range of 1.5 to 3 years for the skeletally immature animals used in the present study.

Shaft Length and Sectioning

After initial storage at −20°C, and subsequent placement in 70% ethyl alcohol at room temperature (20°C), all calcanei were measured and cut into segments according to previously described methods (Skedros et al., 1994a). Briefly, the calcaneal diaphyseal "length" of each bone was defined and measured using a vernier caliper (Fig. 1). Transverse cuts were made along the body of the calcaneus producing 5- to 6-mm-thick segments at 20, 30, 40, 50, 60, 70, and 80% of the defined "length," the 80% segment being closest to the joint surface. One calcaneus from each pair was used for cortical thickness and ash measurements, and a sample from the paired contralateral calcanei were used for microstructural analysis (described below).

Cortices and Cortical Regions: Terminology

The compression cortex is defined as being cranial to, and the tension cortex caudal to, the medullary canal. In contrast to past studies, the intracortical "envelopes" (pericortical, middle, endocortical) will be referred to as "regions" (periosteal, middle, endosteal) (Skedros et al., 1994a,b). This nomenclature is consistent with Skedros et al. (1996, 1997) and reduces confusion with the four modeling/remodeling "envelopes" used in Frost's Mechanostat paradigm (i.e., periosteal surface, intracortical, cortical endosteal surface, and trabecular) (Burr, 1992; Frost, 1990a,b; Martin and Burr, 1989).

Mineral Content (Percent Ash)

A coring drill bit, a high-speed drill press, and continuous water irrigation were used to obtain 2.5-mm diameter, cylindrically shaped cores of cortical bone from the cranial and caudal aspects of each segment. Cores were removed from within 1 to 4 mm of the subperiosteal surface along the cranial-most and caudal-most margins of each segment. The immediate subperiosteal and subendosteal bone regions were avoided so that fibrous tissue associated with the periosteum (cranial cortex), plantar ligament insertion (caudal cortex), or endosteum, which would artifactually lower mineral content, was not sampled. Since the cortical bone at the 20 and 30% segments was typically thin (< 2.5 mm), the cores from these segments consisted mostly of low porosity cancellous bone, which represented regions of intersection between cranial and caudal trabecular tracts. These cores were meticulously cleaned of soft tissue. Cores were also obtained from the medial and lateral cortices of the 30 and 60% segments.

The method used for determining mineral content by ashing is described in a previous study (Skedros et al.,1993c). Mineral content is calculated by dividing the weight of the ashed bone (W_{AB}) by the weight of the dried, defatted bone (W_{DB}), and multiplying this quotient by 100 [$(W_{AB}/W_{DB}) \cdot 100$].

Cortical Thickness

Subperiosteal thickness of cranial, caudal, medial, and lateral cortices was measured with a vernier caliper. Medial and lateral cortical thickness was measured midway between cranial and caudal medullary surfaces. Subperiosteal cranial-caudal heights and medial-lateral widths of each segment were also measured; medial-lateral width was measured midway between the cranial and caudal endosteal margins of the medullary canal.

Microstructure

Microstructural analyses were conducted on the distal cut surfaces of the 50 and 70% segments (Skedros et al., 1994a) from each of 10 immature and 10 skeletally mature bones. These segments were embedded in polymethyl methacrylate (Emmanual et al., 1987) and prepared for imaging in the backscattered electron (BSE) mode of a scanning electron microscope (Skedros et al., 1993b,c). One non-overlapping 50× image (1.6 × 2.3 mm) and two 100× (0.8 × 1.1 mm) images were obtained in each periosteal, middle, and endosteal region of each tension and compression cortex. Similarly, one 50× and two 100× images were also obtained in each of the medial and lateral cortices midway between the cranial and caudal endosteal margins of the medullary canal. Circumferential lamellar bone was not included in any of the BSE images. The thickness of the circumferential lamellar bone, if present, was recorded using an additional BSE image.

Using conventional point counting techniques and methods described by Skedros et al. (1994b), fractional area of secondary osteonal bone (osteonal bone per area, On.B/Ar) and population densities of new remodeling events (NREs = resorption spaces and newly forming secondary osteons) were determined in each 50× image. Newly forming secondary osteons are defined as those with relatively poorly mineralized bone, seen as relatively darker gray levels in the BSE images (Skedros et al., 1993a,b) and less than one-half of complete radial closure (Skedros et al., 1997). Secondary osteon population density (number of secondary osteons per area, N.On/Ar; no./mm^2), mean area per secondary osteon (On.Ar, mm^2), and porosity were determined in each 100× image (Skedros et al., 1994b).

The On.B/Ar was defined as the total area of secondary bone (S) divided by the total area of secondary bone plus interstitial bone (I), [S/(S+I)]. Since the tension and compression cortices are highly remodeled (Skedros et al., 1994b), the small amount of nonsecondary osteon bone that could be confidently considered primary (< 5% of the area of any image) was not considered separately, but was considered to be part of the interstitium.

Circumferential Lamellae and Resorption Surfaces

The thickness of regional circumferential lamellar bone was measured to determine if bone modeling, via subperiosteal apposition, had occurred and remained in situ unremodeled. The thickness of circumferential lamellar bone was sampled at 50× magnification at the apical (cranial-most) portion of the cranial cortex. Measurements were made on each image using a vernier caliper. Similar measurements were not made on the tension cortex and other regions since such subperiosteal circumferential lamellae were not seen.

All endosteal and periosteal surfaces were also examined for evidence of resorption activity. Such activity was inferred by the presence of scalloped margins that are indicative of osteoclastic surface resorption. During increases in size of the calcaneal shaft, resorption would be expected along the endosteal cortices. Endosteal resorption at the later stage of development, represented by the sample examined in this study, was predicted (Table 1) to be occurring only along the cranial cortex.

Statistical/Data Analysis

Means and percentages are reported with ± one standard deviation. Unless otherwise stated, percent differences were calculated with reference to data sets from the cranial, lateral, or combined medial and lateral cortices. For example: [((cranial-caudal)/cranial) · 100], or [((medial-lateral)/lateral) · 100].

Cortical thickness data were evaluated using a one-way analysis of variance (ANOVA) and Fisher's LSD post-hoc test. An alpha level of <0.05 was considered statistically significant. Since the mineral content and microstructural data were not normally distributed, they were examined using a Kruskal-Wallis test and Dunn's Multiple Comparison post-hoc test. The alpha level of <0.05 was adjusted using the Bonferroni-Dunn correction to alpha levels of <0.0033 to <0.0001(as indicated). In a few instances, data sets were fit to second-order polynomial equations. Second-order polynomials were selected since they exhibited superior goodness-of-fit when compared to other regression equations (TableCurve™ v4.00, Jandel Scientific, San Rafael, CA). Regression coefficients and *P*-values for the polynomials were obtained using a commercially available statistical program (StatView Version 5.0, SAS Institute Inc., Cary, NC).

RESULTS

Gross Bone Form, Cross-Sectional Shape, and Bone Length

Both mature and immature bones lack gross longitudinal curvature, and their cross-sections resemble ovoid shapes with the major (elongated) axis oriented in the cranial-caudal direction (Figs. 1 and 3). Examination of all segments of each group showed that cancellous bone tissue was adherent to the cortex in all but the cranial aspect of the 80% segment. The average shaft length of the mature bones is 0.4 cm longer than the average shaft length of the skeletally immature bones (6.51 ± 0.26 cm vs. 6.14 ± 0.29 cm) ($P < 0.001$). Since this difference is small, an attempt to use length to normalize the data did not substantially alter the results.

Height, Width, and Cortical Thickness

At each segment the overall cranial-caudal height of the skeletally mature group was on average 7 ± 2% greater than the cranial-caudal height of corresponding segments of the skeletally immature group (range: 4 to 10% greater; $P < 0.05$ at 20% segment; $P < 0.001$ from 30 to 70% segments; $P < 0.01$ at 80% segment) (Fig. 4). In the 30 to 80% segments of both mature and immature groups, the compression cortex is significantly thicker ($P < 0.001$) than the corresponding tension cortex (Fig. 5). At the 20% segments (near the Achilles tendon), the thicknesses of the compression and tension cortices are not statistically different ($P > 0.05$).

Comparisons between mature and immature groups showed that at each segment from 30 to 80%, the compression cortex of the skeletally mature group was on average 24 ± 10% thicker than the corresponding compression cortex of the immature calcanei ($P < 0.001$ at each segment from 30 to 80%; range 11–46%) (Fig. 5). In contrast, there were no statistically significant inter-group differences in thickness of the tension cortex ($P > 0.05$) (Fig. 5). Also, the minor inter-group difference in the cranial-caudal height of the medullary canal was not statistically significant (3.5% difference, $P > 0.4$). These data, therefore, suggest that overall cranial-to-caudal height increases during maturation primarily by apposition of bone on the compression cortex (Fig. 3).

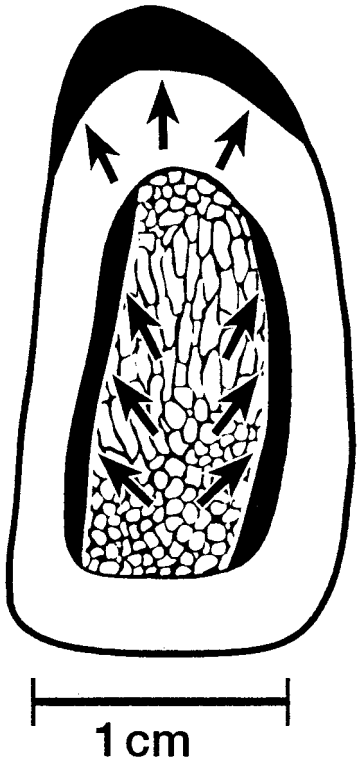

Fig. 3. A representative transverse cross-section from the 50% location of a skeletally mature bone. Arrows and thickened lines indicate the preferential increase in thickness of the compression cortex by periosteal bone accretion, and the equivalent amount of accretion of bone on the endosteal surfaces of the medial and lateral cortices. This drawing demonstrates that with maturation, the cross-section of the calcaneal shaft becomes relatively elongated in the cranial-caudal direction, but there is no change in overall medial-lateral width.

Mean overall medial-lateral width at 50% length was 10.1 ± 1.0 mm in immature bones, and 10.1 ± 0.9 mm in mature bones. There were no statistically significant differences between the two age groups in terms of overall medial-lateral widths from the 30 to 80% segments. However, from the 30 to 70% locations in the mature bones, the medial cortex increased in thickness by 24% ($P < 0.0001$) and the lateral cortex by 20% ($P < 0.0001$). These data suggest that medial and lateral cortices increased in thickness during maturation by endosteal apposition (Fig. 3).

Mineral Content

In the skeletally immature calcanei, the compression cortex had a level of mineralization averaging 8.9% greater than that of the tension cortex ($P < 0.001$) (Table 2). In the skeletally mature calcanei, the compression cortex had a level of mineralization averaging 6.8% greater than in the tension cortex ($P < 0.001$) (Skedros et al., 1994a). The compression cortex of mature bones exhibited a 1.3% average increase in mineral content (range: −1.4 to 3.2%) when compared to the compression cortex of immature bones (Fig. 6). The tension cortex of mature

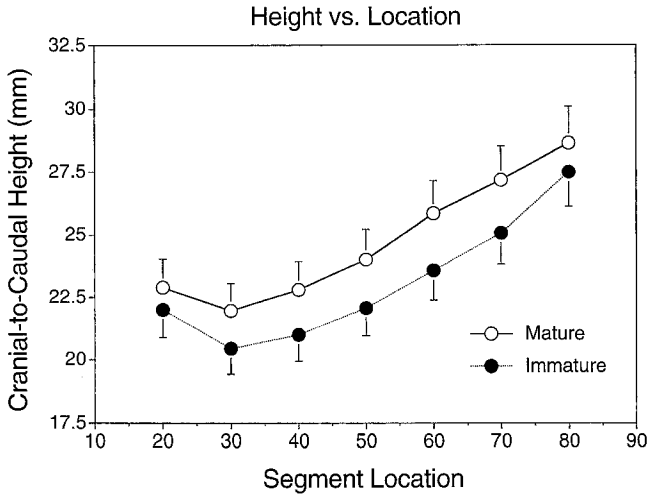

Fig. 4. Plots of mean cranial-caudal height vs. segment location show that in both groups the calcanei progressively elongate in the cranial-caudal direction as the ankle joint is approached. Inspection of the regression lines demonstrates that their slopes are similar, suggesting that increases in cranial-caudal height are isometric during this maturation interval. Bars indicate one standard deviation.

bones exhibited a 3.5% average increase (range: 0.7–4.8%) when compared to the tension cortex of immature bones.

At the 30 and 60% segments, there were no significant mineral content differences ($P > 0.3$) between the medial, lateral, and tension cortices in each age group. Figure 6 shows that mineral content of the tension and compression cortices of both groups generally increases from the 20 to 60% segments, and then decreases at the two most proximal segments. In mature bones, these data show very high correlations when fit to second-order polynomial functions.

Microstructure: Tension vs. Compression Cortices

In immature bones, no significant difference in N.On/Ar was found between tension and compression cortices ($P = 0.97$) (Tables 2 and 3; Fig. 7a–d). However, the compression cortex of the immature bones has 35.0% lower On.B/Ar ($P < 0.0001$) and 51.4% lower porosity ($P < 0.0001$) than the tension cortex. The higher On.B/Ar but equivalent N.On/Ar can be partially attributed to generally larger osteon cross sectional areas in the tension cortex compared to the compression cortex (Tables 2 and 3, Fig. 7a,b,d). In mature bones, the compression cortex has 11.4% greater N.On/Ar ($P < 0.01$), 14.2% lower On.B/Ar ($P < 0.01$), and 44.7% lower porosity ($P < 0.01$) than the tension cortex. The inter-group differences for the compression and tension cortices are [mature vs. immature = ((mature-immature)/mature) · 100]: (1) mature compression vs. immature compression (mature> immature in all cases): 20.1% N.On/Ar ($P = 0.016$), 39.6% On.B/Ar ($P < 0.0001$), 13.7% porosity ($P = 0.052$), and 4.5% osteon area ($P = 0.70$); (2) mature tension vs. immature tension (mature>immature in all cases): 11.4% N.On/Ar ($P = 0.07$), 22.8% On.B/Ar ($P < 0.0001$), 0.75% porosity ($P = 0.91$), and 10.7% osteon area ($P = 0.13$).

Microstructure: Medial vs. Lateral Cortices

In immature bones, medial vs. lateral differences are not significantly different (Tables 2 and 3; Fig. 7a–d). In mature bones some of the medial vs. lateral differences are significantly different (medial>lateral in N.On/Ar, On.B/Ar, and porosity): 59.5% N.On/Ar ($P = 0.001$), 29.3% On.B/Ar ($P = 0.052$), 7.9% porosity ($P = 0.33$), and −28.5% osteon area ($P = 0.01$). The inter-group differences (mature vs. immature) in the medial and lateral cortices are: (1) medial vs. medial differences (mature>immature in N.On/Ar and On.B/Ar): 26.9% N.On/Ar ($P = 0.03$), 21.5% On.B/Ar ($P = 0.07$), −29.4% porosity ($P = 0.008$), and −11.8% osteon area ($P = 0.18$); (2) lateral vs. lateral differences (mature>immature in N.On/Ar, On.B/Ar, and osteon area): 3.0% N.On/Ar ($P = 0.86$), 16.8% On.B/Ar ($P = 0.26$), −35.3% porosity ($P = 0.002$), and 9.1% osteon area ($P = 0.48$).

Microstructure

Intracortical Regions: Tension and Compression Cortices. Immature and mature calcanei demonstrated no significant differences between the periosteal and middle regions in either the tension or compression cortices (Table 3). In contrast, *P*-values listed in Table 3 show that the endosteal regions in only the compression cortex of immature bones and the endosteal regions of the compression and tension cortices of mature bones generally have lower N.On/Ar, higher On.B/Ar, and larger osteon areas than the adjacent middle and periosteal regions. Further, porosity of endosteal regions tends to be higher only in the tension cortices of the immature and mature bones (Fig. 7).

Inter-group differences (mature vs. immature) between the regions of the compression cortex include: 1.) periosteal vs. periosteal differences (mature>immature in all cases): 22.3% N.On/Ar ($P = 0.002$), 32.7% On.B/Ar ($P < 0.0001$), 13.4% porosity ($P = 0.55$), and 11.8% osteon area ($P = 0.72$); 2.) middle vs. middle differences (mature>immature in all cases): 11.4% N.On/Ar ($P = 0.14$), 37.1% On.B/Ar ($P < 0.0001$), 6.7% porosity ($P = 0.77$), and 33.3% osteon area ($P = 0.14$); 3.) endosteal vs. endosteal differences (mature>immature in all but osteon area): 33.8% N.On/Ar ($P = 0.047$), 51.5% On.B/Ar ($P < 0.0001$), 19.2% porosity ($P = 0.40$), and −9.1% osteon area ($P = 0.36$).

Inter-group differences (mature vs. immature) in the regions of the tension cortex include: 1.) periosteal vs. periosteal differences (mature>immature in N.On/Ar and On.B/Ar): 25.6% N.On/Ar ($P = 0.01$), 30.3% On.B/Ar ($P < 0.0001$), −34.5% porosity ($P = 0.11$), and −4.3% osteon area ($P = 0.87$); 2.) middle vs. middle differences (mature>immature in N.On/Ar and On.B/Ar): 12.2% N.On/Ar ($P = 0.20$), 19.7% On.B/Ar ($P < 0.0001$), −11.7% porosity ($P = 0.50$), and 0.0% osteon area ($P = 0.95$); and 3.) endosteal vs. endosteal differences (mature>immature in all but N.On/Ar): −10.8% N.On/Ar ($P = 0.43$), 19.8% On.B/Ar ($P < 0.0001$), 24.1% porosity ($P = 0.005$), and 28.6% osteon area ($P = 0.01$).

New Remodeling Events (NREs = Resportion Spaces Plus Newly Forming Osteons)

Tension cortices in each group had greater numbers of NREs than the compression cortices (immature 349.1%, $P < 0.0001$; mature 409.2%, $P = 0.0003$) (Tables 2–3; Fig. 7e). Also, the compression cortices of immature bones had nearly eightfold more NREs than the compression cortices of mature bones ($P = 0.0012$), and there were nearly sevenfold more NREs in the tension cortices of immature

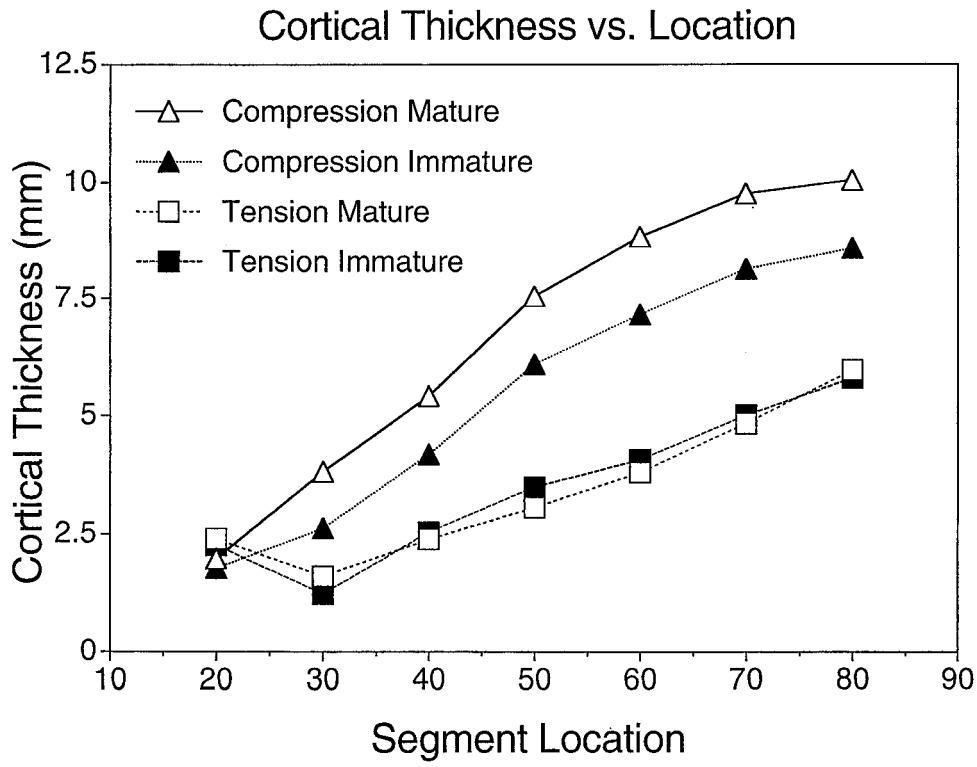

Fig. 5. At top are plots showing means of compression cortical thickness vs. segment location for both groups. These regression lines demonstrate that the thickness of the compression cortex increases in this maturation interval. At bottom are plots showing means of tension cortical thickness vs. segment location for both groups. Inspection of the regression lines demonstrates that their slopes are similar, showing that the thickness of the tension cortices remains essentially unchanged in this maturation interval.

bones than in the tension cortices of mature bones ($P < 0.0001$). Figure 7e shows that in the compression cortices, there were more NREs in the periosteal regions of immature bones compared to periosteal regions of mature bones ($P = 0.0004$). Differences in the middle and endosteal intracortical regions were not statistically significant in both age groups. In contrast, Figure 7e shows that in the tension cortices the number of NREs in the immature bones exceeds that of the respective regions in the mature bones ($P < 0.0001$). No significant differences in NREs were found between the medial and lateral cortices within ($P > 0.75$) and between ($P > 0.11$) the two groups.

Microstructure

Tension and Compression Cortices vs. Medial +Lateral Data. In each group, N.On/Ar of the compression cortex is greater than the mean of combined N.On/Ar data of the medial and lateral cortices (immature 112.2% $P < 0.0001$; mature 117.1% $P < 0.0001$). N.On/Ar data of the tension cortices is also greater ($P < 0.0001$) than the medial plus lateral N.On/Ar of each group (immature 111.2% $P < 0.0001$; mature 94.8% $P < 0.0001$).

Similarly, in each group On.B/Ar of the compression cortex is greater than the mean of combined On.B/Ar data of the medial and lateral cortices (immature 66.2% $P < 0.0001$; mature 129.1% $P < 0.0001$). The mean of the combined On.B/Ar data in the tension cortex is greater than the combined On.B/Ar data of the medial and lateral cortices in each group (immature 155.9% $P < 0.0001$; mature 167.0% $P < 0.0001$).

In each group, porosity of the compression cortex is greater than the mean of combined porosity data of the medial and lateral cortices (immature 46.7% $P = 0.07$; mature 124.4% $P = 0.0002$). The porosity of the tension cortex in each group is greater than the mean of combined porosity data of the medial and lateral cortices (immature 202.2% $P < 0.0001$; mature 304.3% $P < 0.0001$).

Population density of NREs in the compression cortex is significantly greater than the mean of combined NREs of the medial and lateral cortices in only the immature group (immature 38.4% $P = 0.002$; mature 116.5% $P = 0.84$). In contrast, the mean of combined NRE data of the tension cortex is much greater than the mean of combined NREs of medial and lateral cortices in each group (immature 526.3% $P < 0.0001$; mature 1,002.6% $P = 0.087$).

Circumferential Lamellae and Resorption Surfaces

Circumferential lamellar bone was detected in the compression cortices of all segments of both groups. No circumferential lamellar bone was seen in the tension cortices of either group. In the compression cortices, the thickness of circumferential lamellar bone is 0.43 ± 0.13 mm in mature bones and 0.38 ± 0.17 mm in immature bones, and this difference is not statistically significant ($P > 0.4$).

TABLE 2. Cortical thickness, mineral content, and microstructure*

	Ct.Th		%ASH		N.On/Ar		On.B/Ar		Po/Ar		On.Ar		NREs	
	Mean	S.D.	Mean	S.D.	Mean	S.D.	Mean	S.D.	Mean	S.D.	Mean	S.D.	Mean	S.D.
Mature														
Compression	6.7	3.0	70.0	3.5	38.1	15.1	69.5	10.5	4.7	2.0	0.022	0.01	0.02	0.04
Tension	3.4	1.6	65.6	4.4	34.2	9.6	83.7	5.9	8.4	5.9	0.028	0.01	0.08	0.13
P-value	<0.0001		<0.001		0.1		<0.0001		<0.0001		0.004		0.0003	
Mature														
Medial	2.3	0.7	68.5	4.0	21.4	8.1	35.3	12.7	2.2	0.5	0.017	0.01	0.00	0.02
Lateral	2.1	0.5	67.6	4.6	13.4	6.5	27.3	12.6	2.0	0.5	0.022	0.01	0.01	0.05
P-value	0.03		>0.35		0.001		0.1		0.3		0.01		0.91	
Immature														
Compression	5.5	2.6	69.1	3.4	30.5	18.2	42.0	17.4	4.1	1.4	0.021	0.02	0.14	0.22
Tension	3.5	1.8	63.5	4.6	30.3	12.4	64.6	13.0	8.3	4.2	0.025	0.01	0.65	0.42
P-value	<0.0001		<0.001		0.97		<0.0001		<0.0001		0.32		<0.0001	
Immature														
Medial	1.9	0.8	68.0	2.7	15.7	8.8	27.7	12.6	2.8	0.9	0.019	0.01	0.09	0.12
Lateral	1.8	0.6	67.6	3.6	13.0	7.3	22.7	12.2	2.7	0.7	0.020	0.01	0.11	0.16
P-value	0.2		>0.35		0.3		0.2		0.7		0.76		0.75	
Compression														
Mature	6.7	3.0	70.0	3.5	38.1	15.1	69.5	10.5	4.7	2.0	0.022	0.01	0.02	0.04
Immature	5.5	2.6	69.1	3.4	30.5	18.2	42.0	17.4	4.1	1.4	0.021	0.02	0.14	0.22
P-value	0.001		0.06		0.02		<0.0001		0.05		0.70		<0.0001	
Tension														
Mature	3.4	1.6	65.6	4.4	34.2	9.6	83.7	5.8	8.4	5.9	0.028	0.01	0.08	0.13
Immature	3.5	1.8	63.5	4.6	30.3	12.4	64.6	13.0	8.3	4.2	0.025	0.01	0.65	0.42
P-value	>0.4		<0.001		0.07		<0.0001		0.9		0.13		<0.0001	
Medial														
Mature	2.3	0.7	68.5	4.0	21.4	8.1	35.3	12.7	2.2	0.5	0.017	0.01	0.00	0.02
Immature	1.9	0.8	68.0	2.7	15.7	8.8	27.7	12.6	2.8	0.9	0.019	0.01	0.09	0.12
P-value	<0.0001		>0.4		0.03		0.07		0.008		0.18		0.16	
Lateral														
Mature	2.1	0.5	67.6	4.6	13.4	6.5	27.3	12.6	2.0	0.5	0.022	0.01	0.01	0.05
Immature	1.8	0.6	67.6	3.6	13.0	7.3	22.7	12.2	2.7	0.7	0.020	0.01	0.11	0.16
P-value	<0.0001		>0.4		0.9		0.3		0.002		0.48		0.11	

*Ct.Th = cortical thickness (cm); %ASH = percent ash; N.On/Ar = secondary osteon population density (no./mm^2); On.B/Ar = fractional area of secondary bone × 100; Po/Ar = fractional area of porous spaces × 100; On.Ar = mean area per secondary osteon (mm^2); NREs = new remodeling events (resorption spaces + newly forming osteons). The "Compression" (cranial) and "Tension" (caudal) mean values for the microstructural data include data from all regions within the respective cortex. The *P*-value represents the results of the comparison; $P < 0.05$ is considered statistically significant. Tension/compression cortical thickness and ash data are from all segments; Medial/lateral cortical thickness data are from all segments; medial and lateral ash data are from the 30 and 60% segments only. Percent difference in mineral content was calculated according the following example: If mineral content is 70% in a sample of compression bone and 67% in tension bone, then the difference is reported as 4.5% greater in the compression bone as compared to the tension bone [((70-67)/67)×100]. Percent differences between pairwise comparisons of data sets from immature (I) and mature (M) groups are made with reference to mature bones [((M-I)/M)×100].

No evidence of recent resorption activity was detected on any endosteal or periosteal surfaces.

DISCUSSION

Mechanostat Paradigm: Strengths and Weaknesses, and Use of a Simple Model for Rigorous Testing

Although there are some notable exceptions (see asterisks in Table 1), the quantitative data presented in this study are generally consistent with Frost's *predicted* outcomes of modeling and remodeling activities in a maturing "tension/compression" bone. The main support for these predictions are the differences between the "tension" (caudal) and "compression" (cranial) cortices, where the compression cortex is thicker and has notably higher mineral content, lower porosity, higher N.On/Ar, and smaller secondary osteons. Inconsistencies with these predictions include: 1.) the microstructural differences between the presumably similarly loaded medial and lateral cortices, and 2.) the lack of increased porosity and remodeling activity in the medial and lateral cortices. However, using an in vitro loading model of the functionally loaded mule deer calcaneus, Su et al. (1999) concluded that the medial and lateral cortices are: 1.) subject to markedly different strain environments as a result of a characteristically oblique neutral axis, and 2.) subject to relatively high strains that are oblique to the longitudinal diaphyseal axis. Implications of these recent strain data, in the context of specific structural and material variations reported herein, are discussed below in subsequent sections. Additionally, as discussed below, the location(s) of surface resorption activities may be inconsistent with the predictions. The first portion of the following discussion summarizes selected literature on the Mechanostat paradigm. This summary is considered in view of a potential role for the artiodactyl calcaneus as an experimental model for testing assumptions and mechanisms of this paradigm.

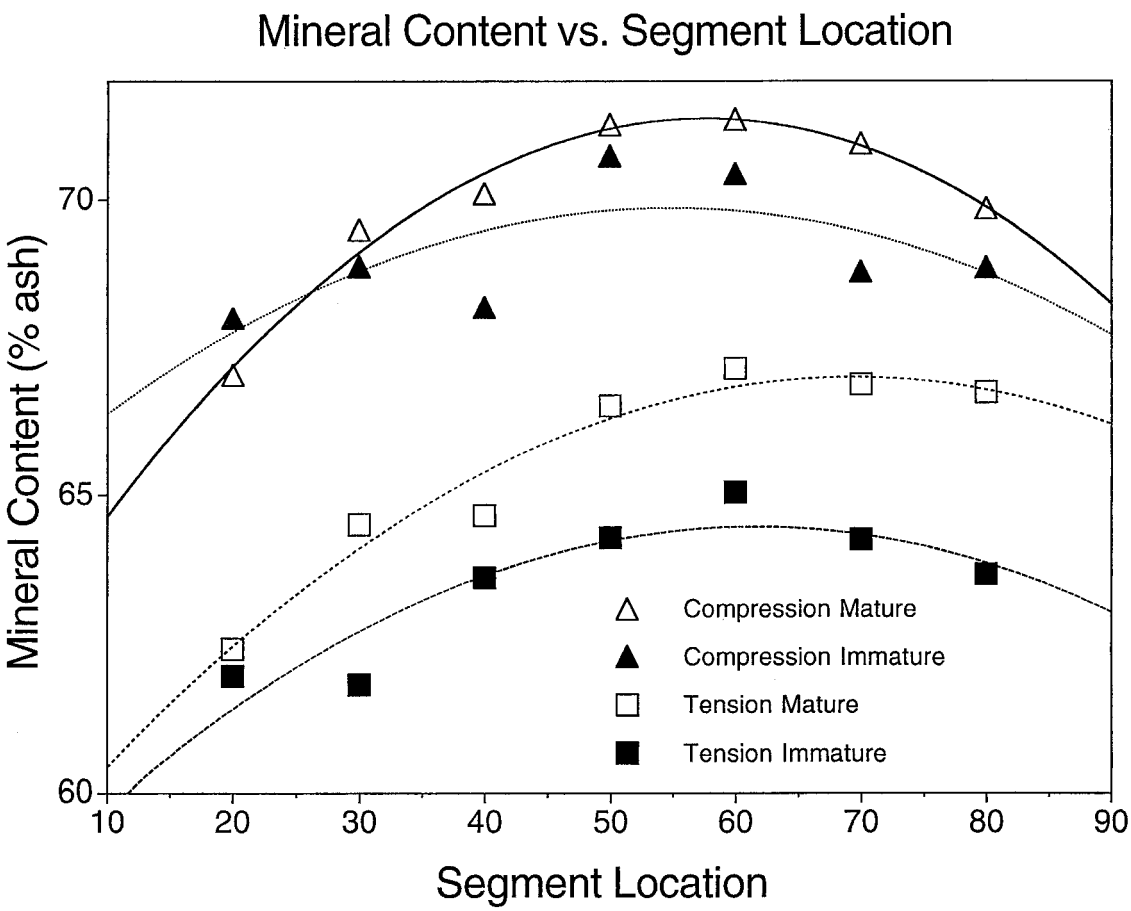

Fig. 6. Mean mineral content vs. mean segment location data fit to second-order polynomial functions: compression mature $y = 61.51 + 0.343\times - 0.003\times^2$, $r^2 = 0.978$, $P < 0.001$; compression immature $y = 64.65 + 0.190\times - 0.002\times^2$, $r^2 = 0.491$, $P = 0.26$; tension mature $y = 57.99 + 0.260\times - 0.002\times^2$, $r^2 = 0.954$, $P = 0.002$; tension immature $y = 57.68 + 0.221\times - 0.008\times^2$, $r^2 = 0.834$, $P = 0.03$. It has been suggested that these distal-to-proximal curvilinear patterns reflect distributions of stress/strain magnitudes along the calcaneal diaphysis. If this interpretation is correct, then the relatively "pure" beam-like portion of the diaphysis is from the distal sections (20–30%) to the 60% section (Skedros et al., 1994a). Note: Minor typographical errors were made in Table 1 of Skedros et al. (1994a). For this reason, the percent differences reported in Figure 6 show minor disparities when compared to those in Table 1 of Skedros et al. (1994a).

Retrospective (Post-Hoc) Analysis of Bone Organization as a Means for Deciphering Strain History

Whether or not the structural/material variations quantified in the mule deer calcaneus are causally related to specific features of local strain histories can not be determined from the present retrospective analysis. This question must be addressed with in vivo strain data quantified in controlled studies of musculoskeletal development. However, numerous studies support the hypothesis that bone tissue is responsive to its strain history (Burr, 1992; Carter et al., 1980; Carter, 1984, 1987; Lanyon and Baggott, 1976; Levenston et al., 1994; Reilly et al., 1997; Riggs et al., 1993a,b; Skedros et al., 1996; van der Meulen et al., 1996). Thus, the hierarchical organization of bone tissue may embody a record or "memory" of important aspects of past and/or current loading conditions (Levenston et al., 1994; Mason et al., 1995; Riggs et al., 1993a,b; Skerry et al., 1990; Skedros et al., 1994a,b, 1996, 1998; Takano et al., 1999). It has been suggested that variations in cortical morphology would be most evident in diaphyses customarily loaded in bending (Skedros et al., 1996, 1997). This is because the mechanical properties, and fracture and microdamage mechanics of cortical bone markedly differ in tension, compression, and shear (Burr et al., 1998; Burstein et al., 1972, 1976; Carter and Hayes, 1977; Cezayirlioglu et al., 1985; Huja et al., 1999; Martin, 1995; Norman et al., 1995, 1996; O'Connor et al., 1982; Pattin et al., 1996; Reilly and Burstein, 1974, 1975). Consequently, a compelling case can be made for examining a "tension/compression" bone for inferring causal relationships between local strain histories and limb bone organization. The results of the present study and past studies also support the use of the artiodactyl calcaneus model for retrospective *and* prospective analyses since it: 1.) has relatively simple and predictable habitual loading environments and strain distributions (Lanyon, 1974; Su et al., 1999), 2.) has unusually heterogeneous material characteristics (mineral content, microstructure, and ultrastructure) *within* the same bone section, 3.) has extensive, and regionally variable, secondary osteon remodeling activities and/or characteristics (in contrast to the rat model, for example, which does not typically exhibit secondary osteon remodeling until extremely advanced age), and 4.)

TABLE 3. *P*-values for comparisons of periosteal (P), middle (M), and endosteal (E) regions within each cortex*

	P vs. M	P vs. E	M vs. E
Immature			
Tension			
N.On/Ar	0.48	0.74	0.27
On.B/Ar	0.05	0.31	0.26
Po/Ar	0.61	0.072	0.013
On.Ar	0.72	0.78	0.95
NREs	0.0025	**0.0001**	**0.0002**
Compression			
N.On/Ar	0.53	**0.0001**	**0.0001**
On.B/Ar	0.17	**0.0001**	**0.0001**
Po/Ar	0.71	0.98	0.76
On.Ar	0.41	**0.0001**	**0.0001**
NREs	0.0075	0.02	0.7
Mature			
Tension			
N.On/Ar	0.33	**0.0001**	**0.0001**
On.B/Ar	0.68	0.15	0.06
Po/Ar	0.48	**0.0001**	**0.0001**
On.Ar	0.57	0.0015	0.007
NREs	0.5	0.99	0.5
Compression			
N.On/Ar	0.25	**0.0001**	**0.0001**
On.B/Ar	0.44	**0.0001**	**0.0001**
Po/Ar	0.46	0.95	0.55
On.Ar	0.7	**0.0001**	**0.0001**
NREs	0.9	0.7	0.8

**P*-value represents one-way ANOVA with Bonferroni Dunn post-hoc comparisons. $P < 0.0004$ is considered statistically significant (bold print). See Table 2 for abbreviations.

is amenable to analyses using multiple rosette strain gauges.

Martin and Burr (1989) have shown that the Mechanostat paradigm is useful for evaluating correlations between bone development, structural/material organization, and strain history. We support this opinion since, in contrast to other modern algorithms of mechanically induced bone adaptation, the Mechanostat paradigm predicts site-specific modeling and intracortical remodeling activities such as the regional microstructure and mineral content heterogeneity quantified in the mule deer calcanei examined in this study. Although other extensive algorithms of mechanobiologic responses in bone are, in many cases, relatively more experimentally tested and/or mathematically developed, they emphasize or only consider *modeling*-related activities, including changes in bone girth, shape, cortical thickness, trabecular orientation, and/or apparent density (Burr, 1992; Carter et al., 1996, 1998; Cowin, 1993; Fyhrie and Schaffler, 1995; Hart and Davy, 1989; Huiskes and Hollister, 1993; Huiskes et al., 1987; Levenston et al., 1994; Martin and Burr, 1989; McNamara et al., 1992; Mullender and Huiskes, 1995).[2] Consequently, Frost's paradigm provides a more useful prospective framework for interpreting the results of the present study since it explicitly attempts to link specific bone-cell activities to biomechanical conditions by clearly distinguishing between modeling *and* remodeling processes, and thresholds for activating primary lamellar, woven, or secondary osteonal bone (Duncan and Turner, 1995; Hoshaw et al., 1994; Martin and Burr, 1989; Martin et al., 1998; Turner, 1991).

Support for the Mechanostat Paradigm, and Its Role as a Set of "Working Hypotheses"

Previous studies show examples of bone modeling and/or remodeling in adult animals that seem consistent with the Mechanostat paradigm (reviewed by Forwood and Turner, 1995; Mosley et al., 1997; Rubin and Lanyon, 1985; Turner et al., 1995). Additionally, investigators have found portions of this paradigm a useful framework for understanding and evaluating intercellular communication among bone cells via gap junctions (Donahue, 1998) and responses of bone to exercise, immobilization, underloading, overloading, functional loading, post-menopausal estrogen deficiency, some pathologic conditions, corrective osteotomies, and implanted orthopaedic and dental prosthetic devices (Aloia, 1993; Bouvier and Hylander, 1996; Boyle, 1993; Brand, 1997; Burr, 1992; Burr and Martin, 1989; Erben, 1996; Ferretti et al., 1998; Frost, 1997, 1998a; Garetto et al., 1995; Hoshaw et al., 1994; Huiskes et al., 1992; Isidor, 1997; Jaworski, 1987; Jee and Frost, 1992; Jee et al., 1991; King et al., 1991; Lanyon, 1996a; Lerner et al., 1998; Marotti, 1996; Martin and Burr, 1989; Mason et al., 1995; Rodriguez et al., 1988; Skedros et al., 1994a,1994b, 1997; Snow, 1996; Taylor, 1997; Thomas et al., 1996; Turner et al., 1995; van Rietbergen et al., 1993). (See Lanyon, 1996b, for further discussion of the error-strain hypothesis of bone organ homeostasis.)

Experimental Data Not Consistent With the Mechanostat Paradigm

Recent experimental studies using an in vivo rat limb bone model exposed to controlled loads have shown that the mechanical stimuli involved in lamellar bone formation are not limited to the peak strain magnitude defined in the general Mechanostat hypothesis (Forwood and Turner, 1995; Mosley and Lanyon, 1998). Bouvier and Hylander (1996) have reported remodeling activities in facial bones of normal and diet-manipulated macaques that are not entirely consistent with predictions of Frost's paradigm. Additionally, several authors have reviewed results of studies of adaptive changes in bone that are mediated by strain features that are not consistent with this paradigm (Lanyon, 1996a; Martin and Burr, 1989; Turner, 1998). Ontogenetic studies of strain distributions and magnitudes on chick limb bones also question the idea that surface-specific modeling activity is an error-driven response to high strains (Biewener and Bertram, 1993a). Although some criticisms (e.g., Turner, 1999) may be spurious (Frost, 2000a), there are many others that can only be addressed by hypothetical-deductive experimentation.

Clarifying the Limits of the Mechanostat Paradigm as an Algorithm for Mechanically Mediated Bone Adaptation: The Role of the Artiodactyl Calcaneus in Experimental Testing

Additional experimental work will be needed to determine whether or not the Mechanostat paradigm will be-

[2]An exception includes Hazelwood, Martin, and coworkers' (Hazelwood, 1998; Hazelwood et al., 1999) advanced computational algorithm of trabecular bone hemi-osteon based adaptation, which includes details of both BMU activity and responses to mechanical loading (see also Huiskes et al., 2000; Martin, 1995).

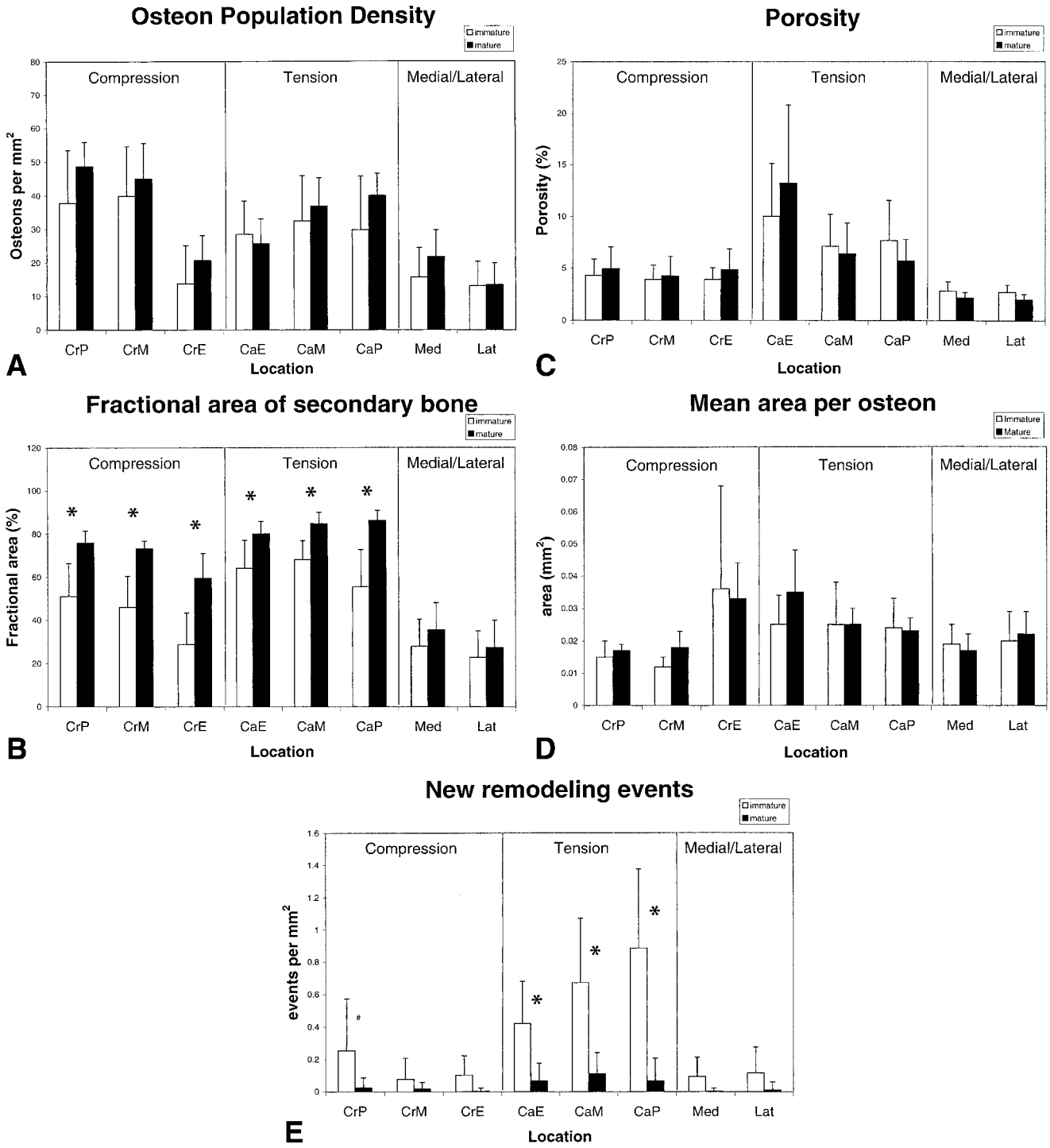

Fig. 7. Microstructural data; means and standard deviations. A: Secondary Osteon Population Density (N.On/Ar). B: Fractional Area of Secondary Bone (On.B/Ar). C: Porosity. D: Mean Area per Secondary Osteon (On.Ar) (including the central canal). E: New Remodeling Events (NREs). Cr = cranial, Ca = caudal, P = periosteal region, M = middle cortical region, E = endosteal region, Med. = medial, Lat. = lateral. **A,B:** No statistically significant differences were found between any of the mature-immature data pairs. In contrast, On.B/Ar comparisons show that there are significant differences (*) in all pairs in both the tension and compression cortices (statistical significance is $P < 0.0001$; this Bonferonni-Dunn correction corresponds to $P < 0.01$ in uncorrected comparisons). The presence of differences in On.B/Ar, but not N.On/Ar, suggests that differences in secondary osteon cross-sectional area and/or number or size of secondary osteon fragments may be present and can influence On.B/Ar but not N.On/Ar. **C,D:** Porosity and osteon cross-sectional area data show no statistically significant differences between any of the *adjacent* mature-immature data pairs. The observation of apparent differences in osteon size in some of these immature-mature data pairs, but the lack of statistical significance, may reflect insufficient statistical power required for showing statistically significant differences. However, on average, osteon cross-sectional areas are significantly larger in the tension cortices (vs. compression cortices) in each age group. **E:** New remodeling event (NRE) data show statistically significant differences between compression periosteal regions (#$P < 0.0004$, Bonferonni corresponding to $P < 0.05$) and between all data pairs in the tension cortices (*$P < 0.0001$, Bonferonni corresponding to $P < 0.01$).

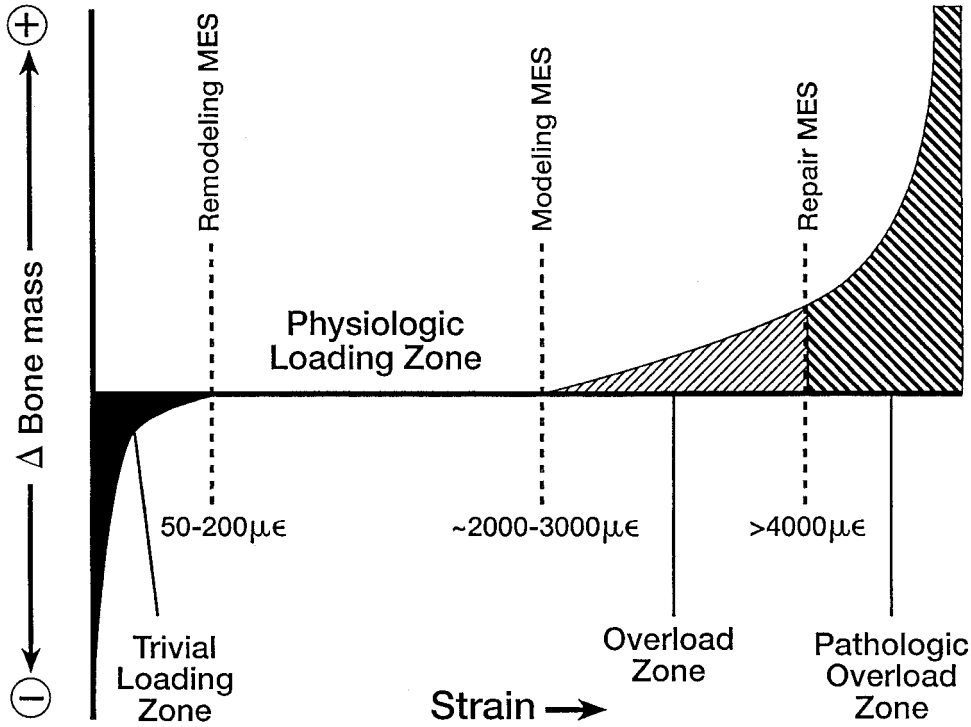

Fig. 8. The four mechanical usage windows or zones, according to the Mechanostat hypothesis. This figure emphasizes that there are differences between thresholds for modeling and remodeling activities. Below the minimum effective strain of remodeling (MESr) (low or "trivial" loading zone), strains are low and bone remodeling is *activated*. Above the remodeling MESr but below the modeling MESm (the physiologic loading zone), remodeling activity is relatively *repressed*, and is also under the influence of hormonal and metabolic influences. [This physiologic loading zone is analogous to the "lazy" zone described by Carter et al. (1996) and "dead" zone described by Huiskes et al. (1992) (see Burr, 1992).] Above the modeling MESm, lamellar bone is gained through increased modeling. Above the repair MESp (pathologic overload zone), new woven bone is added rapidly to bone surfaces; this is neither modeling nor remodeling, but probably represents a repair reaction. Reproduced from Burr (1992) with permission of the publisher.

come an *explanatory* model, which is based on *mechanisms*. This work is necessary since accurate *prediction* of a model does not mean that the model, or its assumptions, are correct (Oreskes et al., 1994). However, depending on its predictive capacity, an algorithm can reveal information about the processes it simulates and generate fruitful hypotheses about underlying mechanisms (Huiskes, 1995). Consequently, inconsistencies between experimental data and the Mechanostat paradigm are not a fatal flaw, but they do narrow the scope of its applicability in skeletal biology. As discussed below, experimental data reported in the present study suggest that the artiodactyl calcaneus may be an appropriate experimental model for examining specific assumptions of this paradigm. The domestic sheep calcaneus may be most useful for comparative studies since it is similar to humans in terms of bone remodeling (Newman et al., 1995; Pastoureau et al., 1989).

Modifications of Cross-Sectional Geometry: Support for Some Predictions of Frost's Paradigm

In Frost's idealized "tension/compression" bone (Fig. 2), the asymmetric modeling activities and the corresponding preferential increase in thickness of the compression cortex presumably represent the means for lowering relatively high tissue strains to within a physiologic range (Fig. 8). Results of the present study demonstrate that cranial-caudal elongation occurs in the mule deer calcaneus primarily by accretion of bone on the periosteal surface of the compression cortex (Figs. 3 and 5). In contrast, there was no evidence of modeling activity on the periosteal surface of the tension cortex. Although increases in the thickness of the tension cortex occur earlier in this bone's development, formation of bone on this cortex had apparently ceased by the stage of maturation represented by the skeletally immature bones in this study. During development, resorption occurs on the periosteal surface of the tension cortex of Frost's idealized "tension/compression" bone. This functions to change bone curvature and is not required in artiodactyl calcanei since their diaphyseal regions are relatively straight in immature and mature animals (Schmid, 1972). Additionally, resorption along the subperiosteal surface of the tension cortex of the artiodactyl calcaneus, if present during ontogeny, would not be expected to persist throughout maturation because this might compromise the anchorage of the plantar ligament, which firmly attaches along the caudal margin of the entire tension cortex (Skedros et al., 1994a,b, 1997; Su et al., 1999) (Fig. 1). In accordance with Frost's bone modeling rules, resorption of the endosteal surface of the cranial cortex was also predicted. Absence of such resorption is inconsistent with these predictions. However, the growth-related modeling activity (i.e., resorption) along the caudal

endosteal surface may have ceased by the stage of growth represented by the immature bones.

Cortical Drift: A Confounding Variable?

Bone formed on a surface early in the development of a long bone may eventually be relocated relative to that surface by cortical drift (coordinated resorption and deposition of bone to effect bone movement through tissue space) (Biewener and Bertram, 1993b; Enlow, 1962a, 1963). For example, as bone apposition on the periosteal surface occurs, areas of tissue that were previously "periosteal," come to lie in the "middle" region. Thus, bone in a given location of a bone section, if recently translocated by cortical drift, could retain the microstructural organization that it had in the location from which it had drifted (Bromage 1992; Enlow, 1962b, 1963). The forces acting on this relocated bone are not necessarily the same forces that acted on the bone during its original formation. Consequently, a "drifted" region that remains unremodeled could confound conclusions about the adaptive relevance of regional variations (Marotti, 1963; Martin and Burr, 1989, pp 53, 158). Results of the present study suggest that the only region that could have recently drifted in the cranial-caudal direction is the subperiosteal margin of the compression cortex. If this is correct, then bone in the middle region of the cranial cortex was probably once closer to the subperiosteal surface. Data showing similar microstructure of the middle and periosteal regions in the compression cortices of each group suggest that the secondary bone in the subperiosteal region, although probably formed and remodeled more recently than the middle region, had likely been in situ for a sufficient amount of time for remodeling to create a microstructure that resembles that of the middle region. These data strengthen the previous suggestions of Skedros et al. (1994a,b) that microstructural organization of the regions within, and mineral content differences between, the tension and compression cortices of mature mule deer calcanei are not remnants of cortical drift.

Cortical Microstructural Variations, Strain Mode, and the Remodeling MES

Reticence of Strain Mode in Frost's Strain-Threshold-Mediated Remodeling Rules. In order to better interpret the present data showing intracortical and surface-related structural/material variations, the modeling and remodeling "rules" of Frost's Mechanostat paradigm must be clarified. More detailed discussion of these rules can be found in Frost (1990a,b) and Burr (1992). The *modeling* rules of the Mechanostat paradigm, although strongly influenced by strain magnitude, are also dependent upon strain mode (or *polarity* = tension, compression, and shear) and changes in relative surface curvature in accordance with Frost's Flexural Neutralization hypothesis (Burr, 1992; Martin and Burr, 1989). *Remodeling* rules, however, are largely reticent of differences in strain mode, being couched primarily in terms of strain magnitudes. According to Frost (Table 1), the activation of bone remodeling that occurs in a normal, healthy, skeletally mature animal is governed by threshold levels of tissue strains defined at a lower limit by a minimum effective strain of remodeling (MESr) and at a higher limit by relatively large strains associated with an increased incidence of microdamage (Fig. 8). Below the MESr, remodeling is activated, and above the MESr, but below the microdamage strains, remodeling is relatively repressed and occurs at a relatively low rate (Frost, 1988a,b, 1990a,b, 1997; Martin and Burr, 1989). This "reticence" to mode is not absolute since site-specific differences in the magnitude of the average MESr may occur; hence, opposing tension and compression cortices may not have the same MESr (Biewener and Bertram, 1993a; Frost, 1990a,b, 2000a) (Fig. 2).

Microstructure and the Theoretical Remodeling Minimum Effective Strain (MESr)

In mature mule deer calcanei, the different microstructure of the endosteal regions, compared to the adjacent middle and periosteal regions, in both tension and compression cortices might be a consequence of increased remodeling activity associated with strains existing below a theoretical MESr (Figs. 2 and 8) (Skedros et al., 1994b). The similar microstructure of adjacent middle and periosteal regions may reflect the repressed remodeling activity in regions where strains exceed the MESr but fall below the high strains that produce microdamage. However, in the compression cortices of immature bones and in the tension and compression cortices of mature bones (Table 3) no statistical differences were found in the number of NREs between the periosteal and endosteal regions, and between middle and endosteal regions. Therefore, the osteon microstructural variations between the endosteal region vs. the periosteal and middle regions are likely better explained by a mechanism other than *active* intracortical renewal (e.g., metabolic influence of nearby marrow) (Frost, 1998a; Marotti, 1996; Martin and Burr, 1989; Skedros et al., 1996).

The relatively few NREs per mm^2 in compression, medial, and lateral cortices of the mature limb bones suggests that these areas have attained the low frequency of remodeling typical of normal mature limb bones (Martin and Burr, 1989). These data are consistent with previous suggestions that quiescent osteon remodeling in the cranial, medial, and lateral cortices may reflect the customary prevalence of relatively high strains in accordance with strain-magnitude-based remodeling rules of the Mechanostat paradigm (Fig. 8). With respect to the medial and lateral (neutral axis) regions, this conclusion seems contradictory since such "neutral axis" regions are considered to be habitually low-strain environments (with increased porosity and remodeling activity, and decreased mineral content). However, our conclusion that these data are not ipso facto contradictory reflects an increased awareness that "neutral axis" regions in bones that are habitually loaded in bending actually receive biomechanically important shear strains in addition to principal strains that are significantly deviate from the diaphyseal longitudinal axis (Demes, 1998; Su et al., 1999; Turner, 2000). (Compare Frost, 2000a, and Turner, 2000, for further discussion about shear strains at the neutral axis.)

In contrast to contradictions in medial-lateral experimental data, the following three findings in the tension cortex support the hypothesis that this region in mature bones is actively remodeling and may exist below a tension remodeling MES: 1.) persistence of relatively lower mineral content in the mature tension cortex, compared with the compression, medial, and lateral cortices (Tables 2 and 3), 2.) persistence of relatively increased NREs in the tension cortex, compared with the other cortices (Tables 2 and 3; Fig. 7e), and 3.) previously proposed stress-reducing effect of the adherent plantar ligament and su-

perficial digital flexor tendon on the tension cortex, which may further reduce ambient strains, strengthening the possibility that this region *chronically exists in a state of relative disuse* (Skedros et al., 1994a,b, 1997) (Fig. 2). However, cortical strain data obtained from in vitro functional loading of the mule deer calcaneus suggest that caudal cortical strains (380 to 940 microstrain) markedly exceed the characteristically low strains that are typically suggested for the hypothetical MESr (< 200 microstrain) (Su et al., 1999). This is not consistent with the Mechanostat hypothesis.[3] Further study of the stimuli that govern these regional remodeling variations is warranted. An experimental design that may be useful for such investigations has been described for the sheep calcaneus (Skerry and Lanyon, 1995; Thomas et al., 1996).

Specifics of Strain-Mode-Related Adaptations Are Not Considered in the Mechanostat Paradigm

It has been suggested that differences in predominant collagen fiber orientation between the compression and tension cortices of calcanei of mule deer and other artiodactyls represent adaptations that are strongly strain-mode-related (Skedros, 1994; Skedros et al., 1994b, 1997, 1999). There are quantitative data showing that the tension cortex has collagen fibers with predominant longitudinal orientation in contrast to the opposing compression cortex, which has comparatively more oblique-to-transverse fibers (Skedros, 1994; Skedros et al., 1998). Differences in predominant orientation of collagen fibers have also been reported between "tension" and "compression" cortices of other limb bones that are subject to customary bending including human proximal femoral diaphyses and mid-diaphyses of sheep radii, horse radii, dog radii, and horse third metacarpals (Lanyon et al., 1979; Mason et al., 1995; Marotti, 1963; Martin et al., 1996a,b; Portigliatti Barbos et al., 1983, 1984; Riggs et al., 1993a,b; Skedros, 1994; Skedros and Kuo, 1999; Skedros et al., 1996, 1999; Takano et al., 1999). If collagen orientation differences represent strain-mode-related adaptation, then these data expose an apparent deficiency of the largely strain-magnitude-based rules of the Mechanostat paradigm.

However, Martin and Burr (1989) emphasize that the rules of the Mechanostat paradigm are governed by two "theories" of bone's mechanically adaptive mechanisms:

> Activation of *remodeling BMUs* is determined by strain levels according to the Mechanostat Theory: disuse increases activation and overstrain reduces it. Once activated, BMUs function according to the Flexural Neutralization Theory (FNT), producing net formation or resorption according to the polarity of the streaming potentials produced by strain gradients. In osteonal remodeling, the latter phenomena comprise what we have called the osteon alignment theory, but this is merely an internal form of the FNT. (Martin and Burr, 1989, pp 211–212.)[4]

Hence, after woven bone is formed, it is replaced by secondary bone via modeling and remodeling processes that are *initiated* by processes described in the general Mechanostat hypothesis and *controlled* (e.g., orientation of BMU migration) by the processes of the Flexural Neutralization Theory (Martin and Burr, 1989). Since the customary orientation of stress and strain trajectories in the artiodactyl calcaneal shaft can be measured (Biewener et al., 1996; Lanyon, 1974; Su et al., 1999), this bone may also provide a useful model for examining mechanisms of osteon construction and orientation.

CONCLUSIONS

- The artiodactyl calcaneus appears useful for examining the cause-effect mechanisms that mediate bone development, maintenance, and adaptation in the context of comprehensive paradigms/algorithms of mechanically mediated bone adaptation.
- This model appears useful for exploring the mechanisms of regional osteopenia associated with apparent rapid osteonal remodeling (i.e., in the caudal calcaneal cortex).
- This model appears useful for determining if bone responds to specific epigenetic stimuli of a physiologic nonuniform strain distribution to create a heterogeneous material organization.
- This model is appealing because distinct regional differences in modeling- and remodeling-mediated characteristics can be found in the same bone cross-section.

ACKNOWLEDGMENTS

We thank Eric G. Vajda and Todd M. Boyce for their reviews of the manuscript, Howard Winet and Harold M. Frost for insightful suggestions, Cathy Saunderson and Angel Skedros for technical work, and Gwenevere Shaw for clerical support.

LITERATURE CITED

Aloia JF. 1993. A colour atlas of osteoporosis. Mosby-Year Book Europe Ltd., Aylesbury, England: Hazell Books, p. 1–128.

Anderson AE. 1981. Morphologic and physiological characteristics. In: Walmo OC, ed. Mule and black-tailed deer of North America. Lincoln: University of Nebraska Press, p 27–97.

Banks, WJ, Epling GP, Kainer RA, Davis RW. 1968. Antler growth and osteoporosis: I. Morphological and morphometric changes in the costal compacta during the antler growth cycle. Anat Rec 162: 387–397.

Beaupre GS, Orr TE, Carter DR. 1990a. An approach for time-dependent bone modeling and remodeling: theoretical development. J Orthop Res 8:651–661.

Beaupre GS, Orr TE, Carter DR. 1990b. An approach for time-dependent bone modeling and remodeling, application: a preliminary remodeling simulation. J Orthop Res 8:662–670.

Bertram JEA, Swartz SM. 1991. The "Law of bone transformation": a case of crying Wolff? Biol Rev 66:245–273.

Biewener AA, Bertram JEA. 1993a. Skeletal strain patterns in relation to exercise and training during growth. J. Exp. Biol., 185:51–69.

Biewener AA, Bertram JEA. 1993b. Mechanical loading and bone growth in vivo. In: Hall BK, editor. Bone, vol. 7: bone growth, B. Boca Raton: CRC Press Inc. p 1–36.

Biewener AA, Bertram JEA. 1994. Structural response of growing bone to exercise and disuse. J Appl Physiol 76:946–955.

Biewener AA, Thomason J, Goodship A, Lanyon LE. 1983a. Bone stress in the horse forelimb during locomotion at different gaits: A comparison of two experimental methods. J. Biomech., 16:565–576.

[3]Frost (2000b) has recently stated that the MESr may be on the order of 400–600 microstrain.

[4]Authors' note: At present there are fluid mechanical alternatives to streaming potentials as the mechanism for stimulating bone cell action (e.g., the stimulation of cell membrane permeability changes) (Burger et al., 1996; Turner, 1998; Weinbaum et al., 1994).

Biewener AA, Thomason J, Lanyon LE. 1983b. Mechanics of locomotion and jumping in the forelimb of the horse (Equus): in vivo stress developed in the radius and metacarpus. J. Zool., London, 201: 67–82

Biewener AA, Swartz SM, Bertram JEA. 1986. Bone modeling during growth: dynamic strain equilibrium in the chick tibiotarsus. Calcif Tissue Int 39:390–395.

Biewener AA, Fazzalari NL, Konieczynski DD, Baudinette RV. 1996. Adaptive changes in trabecular architecture in relation to functional strain patterns and disuse. Bone 19:1–8.

Bouvier M, Hylander WL. 1996. The mechanical or metabolic function of secondary osteonal bone in the monkey *Macaca Fascicularis*. Arch Oral Biol 41:941–950.

Boyle IT. 1993. Secondary osteoporosis. In: Bailliere T, editor. Bailliere's clinical rheumatology. London: Bailliere Tindall 7:515–534.

Brand RA. 1997. Hip osteotomies: a biomechanical consideration. J Am Acad Orthop Surgeon 5:282–291.

Bromage TG. 1992. Microstructural organization and biomechanics of Macaque circumorbital region. In: Smith P, Tchernov E, editors. Structure, function and evolution of teeth. London: Freund Publishing House. p 257–272.

Burger EH, Klein-Nulend J, Semeins CM, Nijweide PJ. 1996. Effects of fluid flow on bone cells in vitro. In: Davidovitch Z, Norton LA, editors. Biological mechanisms of tooth movement and craniofacial adaptation. Boston: Harvard Society for the Advancement of Orthodontics. p 83–89.

Burr DB. 1992. Orthopedic principles of skeletal growth, modeling and remodeling. In: Carlson DS, Goldstein SA, editors. Bone biodynamics in orthodontic and orthopedic treatment. center for human growth and development, vol. 27. Ann Arbor: University of Michigan. p 15–50.

Burr DB, Martin RB. 1989. Errors in bone remodeling: toward a unified theory of metabolic bone disease. Am J Anat 186:186–216.

Burr DB, Turner CH, Naick P, Forwood MR, Ambrosius W, Hasan MS, Pidaparti R. 1998. Does microdamage accumulation affect the mechanical properties of bone? J Biomech 31:337–345.

Burstein AH, Currey JD, Frankel PVH, Reilly DT. 1972. The ultimate properties of bone tissue: effects of yielding. J Biomech 5:35–44.

Burstein AH, Reilly DT, Martens M. 1976. Aging of bone tissue: mechanical properties. J Bone Joint Surg 58-A:82–86.

Carter DR. 1982. The relationship between in vivo strains and cortical remodeling. In: Bourne JR, editor. CRC critical reviews in bioengineering. Boca Raton: CRC Press Inc. p 1–28.

Carter DR. 1984. Mechanical loading histories and cortical bone remodeling. Calcif Tissue Int 36:S19–S24.

Carter DR. 1987. Mechanical loading history and skeletal biology. J Biomech 20:1095–1109.

Carter DR, Hayes WC. 1977. Compact bone fatigue damage: a microscopic examination. Clin Orthop Rel Res 127:265–274.

Carter DR, Smith DJ, Spengler DM, Daly CH, Frankel VH. 1980. Measurements and analysis of in vivo strains on the canine radius and ulna. J Biomech 13:27–38.

Carter DR, Fyhrie DP, Whalen RT. 1987. Trabecular bone density and loading history: Regulation of tissue biology by mechanical energy. J Biomech 20:785–795.

Carter DR, Beaupre GS, Giori NJ, Helms JA. 1988. Mechanobiology of skeletal regulation. Clin Orthop Rel Res 355S:S41–S55.

Carter DR, van der Meulen MCH, Beaupre GS. 1996. Mechanical factors in bone growth and development. Bone 18(Suppl):5S–10S.

Cowin SC. 1984. Mechanical modeling of the stress adaptation process in bone. Calcif Tissue Int 36:S98–S103.

Cowin SC. 1993. Bone stress adaptation models. Trans ASME 115: 528–533.

Currey JD. 1984. The mechanical adaptations of bones. Princeton, NJ: Princeton University Press. p 1–294.

Cezayirlioglu H, Bahniuk E, Davy DT, Deiple KG. 1985. Anisotropic yield behavior of bone under combined axial force and torque. J Biomech 18:61–69.

Demes B. 1998. Use of strain gauges in the study of primate locomotor biomechanics. In: Strasser E, et al., editors. Primate locomotion. New York: Plenum Press. p 237–254

Donahue HJ. 1998 Gap junctional intercellular communication in bone: A cellular basis for the mechanostat set point. Calc Tissue Int 62:85–88.

Duncan RL, Turner CH. 1995 Mechanotransduction and the functional response of bone to mechanical strain. Calcif Tissue Int 57:344–358.

Emmanual J, Hornbeck C, Bloebaum RD. 1987. A polymethyl methacrylate method for large specimens of mineralized bone with implants. Stain Tech 62:401–410.

Enlow DH. 1962a. Function of the Haversian system. Am J Anat 110:269–306.

Enlow DH. 1962b. A study of the post-natal growth and remodeling of bone. Am J Anat 110:79–101.

Enlow DH. 1963. Principles of bone remodeling. Springfield, IL: Charles C. Thomas Publishing. p 1–131.

Erben RG. 1996. Trabecular and endocortical bone surfaces in the rat: modeling or remodeling. Anat Rec 246:39–46.

Ferretti JL, Schiessl H, Frost HM. 1998. On new opportunities for absorptiometry. J Clin Densitom 1:41–53.

Fisher KJ, Jacobs CR, Carter DR. 1995. Computational method for determination of bone and joint loads using bone density distributions. J Biomech 28:1127–1135.

Forwood MR, Turner CH. 1995. Skeletal adaptations to mechanical usage: Results from tibial loading studies in rats. Bone 17(Suppl): 197S–205S.

Frost HM. 1983. The minimum effective strain: a determinant of bone architecture. Clin Orthop Rel Res 175:286–292.

Frost HM. 1986. Intermediary organization of the skeleton, Vols. I and II. Boca Raton: CRC Press Inc. Vol. I p. 267–353; Vol. II p. 43–63.

Frost HM. 1987. Bone "mass" and the "mechanostat": a proposal. Anat Rec 219:1–9.

Frost HM. 1988a. Structural adaptations to mechanical usage. A proposed "three-way rule" for bone modeling. Part I. Vet. Comparative Orthop Traumatol 1:7–17.

Frost HM. 1988b. Structural adaptations to mechanical usage. A proposed "three-way rule" for bone modeling. Part II. Vet Comparative Orthop Traumatol 2:80–85.

Frost HM. 1989 Mechanical usage, bone mass, bone fragility. A brief overview. In: Kleerekoper M, Krane SM, editors. Clinical disorders in bone and mineral metabolism. New York: Mary Ann Liebert. p 15–40.

Frost HM. 1990a. Skeletal structural adaptations to mechanical usage (SATMU): 1. Redefining Wolff's Law: the bone modeling problem. Anat Rec 226:403–413.

Frost HM. 1990b. Skeletal structural adaptations to mechanical usage (SATMU): 2. Redefining Wolff's Law: the remodeling problem. Anat Rec 226:414–422.

Frost HM. 1996. Perspectives: a proposed general model of the "mechanostat" (Suggestions from a new skeletal-biological paradigm). Anat Rec 244:139–147.

Frost HM. 1997. Defining osteopenias and osteoporoses: Another view (with insights from a new paradigm). Bone 20:385–391.

Frost HM. 1998a. On rho, a marrow mediator, and estrogen: Their roles in bone strength and "mass" in human females, osteopenias, and osteoporoses: insights from a new paradigm. J Bone Miner Metab 16:113–123.

Frost HM. 1998b. Changing concepts in skeletal physiology: Wolff's law, the mechanostat and the "Utah paradigm." J Hum Biol 10: 599–605.

Frost HM. 2000a. Letter to the editor. Calcif Tissue Int 67:184–187.

Frost HM. 2000b. Does bone design intend to minimize fatigue failures? A case for the affirmative. J Bone Miner Metab 18:278–282.

Fyhrie DP, Schaffler MB. 1995. The adaptation of bone apparent density to applied load. J Biomech 28:135–164.

Garetto LP, Chen J, Parr JA, Roberts WE. 1995. Remodeling dynamics of bone supporting rigidly fixed titanium implants: a histomorphometric comparison in four species including humans. Implant Dentistry 4:235–243.

Goss RJ. 1983. Deer antlers. regeneration, function, and evolution. New York: Academic Press, Inc. p 1–316.

Grynpas M. 1993. Age and disease-related changes in the mineral of bone. Calcif Tissue Int 53(Suppl 1):S57–S64.

Hart RT, Davy DT. 1989. Theories of bone modeling and remodeling. In: Cowin SC, editor. Bone biomechanics. Boca Raton: CRC Press Inc. p 253–277.

Hazelwood SJ. 1998. A bone adaptation simulation for the femur based on disuse and damage repair. Ph.D. Dissertation. University of California, Davis.

Hazelwood SJ, Martin RB, Rodrigo JJ, Rashid MM. 1999. A mathematical model for bone remodeling. Presented at Int Mech Eng Congr Expo, Nashville, TN.

Hecht A. 1992. Adaptation and compensation as biological principles of medical thinking and action. In: Regling G, editor. Wolff's law and connective tissue regulation. Berlin: Walter de Gruyter. p 39–44.

Hilmann JR, Davis RW, Abdelbaki YZ. 1973. Cyclic bone remodeling in deer. Calc Tissue Res 12:332:330

Hoshaw SJ, Brunski JB, Cochran GVB. 1994. Mechanical loading of Branemark implants affects interfacial bone modeling and remodeling. Int J Oral Maxillofac Implants 9:345–360.

Huiskes R. 1995. The law of adaptive bone remodeling: a case for crying Newton? In: Odgaard A, Weinans H, editors. Bone structure and remodeling. Singapore: World Scientific. p 15–24.

Huiskes R, Hollister SJ. 1993. From structure to process, from organ to cell: recent developments of FE-analysis in orthopaedic biomechanics. Trans ASME 115:520–527.

Huiskes R, Weinans H, Grootenboer HJ, Dalstra M, Fudala B, Slooff TJ. 1987. Adaptive bone-remodeling theory applied to prosthetic-design analysis. J Biomech 20:1135–1150.

Huiskes R, Weinans H, van Rietbergen B. 1992. The relationship between stress shielding and bone resorption around total hip stems and the effects of flexible materials. Clin Orthop Rel Res 274:124–134.

Huiskes R, Ruimerman R, van Lenthe GH, Janssen JD. 2000. Effects of mechanical forces on maintenance and adaptation of form in trabecular bone. Nature 405:704–706

Huja SS, Katona TR, Burr DB, Garetto LP, Roberts WE. 1999. Microdamage adjacent to endosseous implants. Bone 25:217–222.

Isidor F. 1997. Histological evaluation of peri-implant bone at implants subjected to occlusal overload or plaque accumulation. Clin Oral Impl Res 8:1–9.

Jacobs CR, Levenston ME, Beaupre GS, Simo JC, Carter DR. 1995. Numerical instabilities in bone remodeling simulations: the advantages of a node-based finite element approach. J Biomech 28:449–459.

Jaworski ZFG. 1987. Does the mechanical usage (mu) inhibit bone "remodeling?" Calcif Tissue Int 41:239–248.

Jee WSS, Frost HM. 1992. Skeletal adaptations during growth. Triangle (Sandoz) 31:77–88.

Jee WSS, Li XJ, Ke HZ. 1991. The skeletal adaptation to mechanical usage in the rat. Cells Mater (Suppl1):131–142.

King GJ, Keeling SD, Wronski JT. 1991. Histomorphometric study of alveolar bone turnover in orthodontic tooth movement. Bone 12: 401–409.

Lanyon LE. 1974. Experimental support for the trajectorial theory of bone structure. J Bone Joint Surg 56-B:160–166.

Lanyon LE. 1987. Functional strain in bone tissue as an objective, and controlling stimulus for adaptive bone remodelling. J Biomech 20: 1083–1093.

Lanyon LE. 1996a. Using functional loading to influence bone mass and architecture: Objectives, mechanisms, and relationship with estrogen of the mechanically adaptive process in bone. Bone 18(Suppl):37S–43S.

Lanyon LE. 1996b. Why does a mechanism the successfully matches bone strength to bone loading before menopause fail when oestrogen levels decline? In: Compston J, editor. Osteoporosis: new perspectives on causes, prevention and treatment. London: The College. p 135–150.

Lanyon LE, Baggott DC. 1976. Mechanical function as an influence on the structure and form of bone. J Bone Joint Surg 58-B:436–443.

Lanyon LE, Magee PT, Baggott DG. 1979. The relationship of functional stress and strain to the processes of bone remodelling: An experimental study on the sheep radius. J Biomech 12: 593–600.

Lerner AL, Kuhn JL, Hollister SJ. 1998. Are regional variations in bone growth related to mechanical stress and strain parameters? J Biomech 31:327–335.

Levenston ME, Beaupre GS, Schurman DJ, Carter DR. 1993. Computer simulations of stress-related bone remodeling around noncemented acetabular components. J Arthrop 8:595–605.

Levenston ME, Beaupre GS, Jacobs CR, Carter DR. 1994. The role of loading memory in bone adaptation simulations. Bone 15:177–186.

Lewall EF, Cowan IM. 1963. Age determination in black-tailed deer by degree of ossification of the epiphyseal plate in the long bones. Can J Zool 41:629–636.

Marotti G. 1963. Quantitative studies on bone reconstruction, 1. The reconstruction in homotypic shaft bones. Acta Anat 52:291–333.

Marotti G. 1996. The structure of bone tissues and the cellular control of their deposition. Ital J Anat Embryol 101:25–79.

Martin B. 1993. Aging and strength of bone as a structural material. Calc Tissue Int 53(Suppl 1):S34–S40.

Martin RB. 1995. Mathematical model for repair of fatigue damage and stress fracture in osteonal bone. J Orthop Res 13:309–316.

Martin RB, Burr DR. 1989. Structure, function, and adaptation of compact bone. New York: Raven Press. p 1–275.

Martin RB, Mathews PV, Lau ST, Gibson VA, Stover SM. 1996a. Use of circularly vs. plane polarized light to quantify collagen fiber orientation in bone. Trans Orthop Res Soc 21:606.

Martin RB, Mathews PV, Lau ST, Gibson VA, Stover SM. 1996b. Collagen fiber organization is related to mechanical properties and remodeling in equine bone. A comparison of two methods. J Biomech 29:1515–1521.

Martin RB, Burr DB, Sharkey NA. 1998. Skeletal tissue mechanics. New York: Springer-Verlag. 392 pp.

Mason MW, Skedros JG, Bloebaum RD. 1995. Evidence of strain-mode-related cortical adaptation in the diaphysis of the horse radius. Bone 17:229–237.

McNamara BP, Prendergast PJ, Taylor D. 1992. Prediction of bone adaptation in the ulnar-osteotomized sheep's forelimb using an anatomical finite element model. J Biomed Eng 14:209–216.

Mosley JR, Lanyon LE. 1998. Strain rate as a controlling influence on adaptive modeling in response to dynamic loading of the ulna in growing male rats. Bone 23:313–318.

Mosley JR, March BM, Lynch J, Lanyon LE. 1997. Strain magnitude related changes in whole bone architecture in growing rats. Bone 20:191–198.

Mullender MG, Huiskes R. 1995. Proposal for the regulatory mechanism of Wolff's law. J Orthop Res 13:503–512.

Newman E, Turner AS, Wark JD. 1995. The potential of sheep for the study of osteopenia: Current status and comparison with other animal models. Bone 16(Suppl):277S–284S.

Norman TL, Vashishth D, Burr DB. 1995. Fracture toughness of human bone under tension. J Biomech 28:309–320.

Norman TL, Nivargikar SV, Burr DB. 1996. Resistance to crack growth in human cortical bone is greater in shear than in tension. J Biomech 29:1023–1031.

O'Connor JA, Lanyon LE, MacFie H. 1982. The influence of strain rate on adaptive bone remodelling. J Biomech 15:767–781.

Oreskes N, Shrader-Frechette K, Belitz K. 1994. Verification, validation, and confirmation of numerical models in the earth sciences. Science 263:641–646.

Parfitt AM, Mundy GR, Roodman GD, Hughes DE, Boyce BF. 1996. A new model for the regulation of bone resorption, with particular reference to the effects of bisphosphonates. J Bone Miner Res 11: 150–159.

Pastoureau P, Charrier J, Blanchard MM, Biovin G, Dulor JP, Theriez M, Barenton B. 1989. Effects of a chronic GFR treatment on lambs having low or normal birth weight. Domest Anim Endocrin 6:321–329.

Pattin CA, Caler WE, Carter DR. 1996. Cyclic mechanical property degradation during fatigue loading of cortical bone. J Biomech 29:69–79.

Portigliatti Barbos M, Bianco P, Ascenzi A. 1983. Distribution of osteonic and interstitial components in the human femoral shaft with reference to structure, calcification and mechanical properties. Acta Anat 115:178–186.

Portigliatti Barbos M, Bianco P, Ascenzi A, Boyde A. 1984. Collagen orientation in compact bone: II. Distribution of lamellae in the whole of the human femoral shaft with reference to its mechanical properties. Metab Bone Dis Rel Res 5:309–315.
Purdue JR. 1983. Epiphyseal closure in white-tailed deer. J Wildlife Manage 47:1207–1213.
Reilly DT, Burstein AH. 1974. The mechanical properties of cortical bone. J Bone Joint Surg 56-A:1001–1022.
Reilly DT, Burstein AH. 1975. The elastic and ultimate properties of compact bone tissue. J Biomech 8:393–405.
Reilly GC, Currey JD, Goodship AE. 1997. Exercise of young thoroughbred horses increases impact strength of the third metacarpal bone. J Orthop Res 15:862–868.
Riggs CM, Lanyon LE, Boyde A. 1993a. Functional associations between collagen fibre orientation and locomotor strain direction in cortical bone of the equine radius. Anat Embryol 187:231–238.
Riggs CM, Vaughan LC, Evans GP, Lanyon LE, Boyde A. 1993b. Mechanical implications of collagen fibre orientation in cortical bone of the equine radius. Anat Embryol 187:239–248.
Rodriguez JI, Palacios J, Garcia-Alix A, Pastor I, Paniagua R. 1988. Effects of immobilization on fetal bone development. A morphometric study in newborns with congenital neuromuscular diseases with intrauterine onset. Calcif Tiss Int 43:335–339.
Rubin CT, Lanyon LE. 1984. Dynamic strain similarity in vertebrates; An alternative to allometric limb bone scaling. J Theor Biol 107:321–327.
Rubin CT, Lanyon LE. 1985. Regulation of bone mass by mechanical strain magnitude. Calcif Tissue Int 37:411–417.
Rubin CT, Lanyon LE. 1987. Osteoregulatory nature of mechanical stimuli: function as a determinant for adaptive remodeling in bone. J Orthop Res 5:300–310.
Schaffler MG, Burr DB, Jungers WL, Ruff CB. 1985. Structural and mechanical indicators of limb specialization in primates. Folia Primatol 45:61–75.
Schmid E. 1972. Atlas of animal bones: for prehistorians, archaeologists and quaternary geologists. New York: Elsevier Publishing Co. p 1–153.
Skedros JG. 1994. Collagen fiber orientation in skeletal tension/compression systems: a potential role of variant strain stimuli in the maintenance of cortical bone organization. J Bone Miner Res 9(Suppl1):S251.
Skedros JG, Bloebaum RD. 1991. Geometric analysis of a tension/compression system: Implications for femoral neck modeling. Trans Orthop Res Soc 16:421.
Skedros JG, Kuo TY. 1999. Ontogenetic changes in regional collagen fiber orientation suggest a role for variant strain stimuli in cortical bone construction. J Bone Miner Res 14(Suppl 1):S441
Skedros JG, Bloebaum RD, Bachus KN, Boyce TM. 1993a. The meaning of graylevels in backscattered electron images of bone. J Biomed Mater Res 27:47–56.
Skedros JG, Bloebaum RD, Bachus KN, Boyce TM, Constantz B. 1993b Influence of mineral content and composition on graylevels in backscattered electron images of bone. J Biomed Mater Res 27:57–64.
Skedros JG, Ota D, Bloebaum RD. 1993c. Mineral content analysis of tension/compression skeletal systems: Indications of potential strain-specific differences. J Bone Miner Res 8(Suppl):S314.
Skedros JG, Bloebaum RD, Mason MW, Bramble DM. 1994a. Analysis of a tension/compression skeletal system: possible strain-specific differences in the hierarchical organization of bone. Anat Rec 239: 396–404.
Skedros JG, Mason MW, Bloebaum RD. 1994b. Differences in osteonal micromorphologies between tensile and compressive cortices of a bending skeletal system: Indications of potential strain-specific differences in bone microstructure. Anat Rec 239:405–413.
Skedros JG, Mason MW, Nelson MC, Bloebaum RD. 1996. Evidence of structural and material adaptation to specific strain features in cortical bone. Anat Rec 246:47–63.
Skedros JG, Su SC, Bloebaum RD. 1997. Biomechanical implications of mineral content and microstructural variations in cortical bone of horse, elk and sheep calcanei. Anat Rec 249:297–316.
Skedros JG, Hughes PE, Zirovich MD. 1998. Collagen fiber orientation in the turkey ulna supports a role for variant strain stimuli in cortical bone construction. Bone 23(Suppl 5):S437.
Skedros JG, Hughes PE, Nelson K, Winet H. 1999. Collagen fiber orientation in the proximal femur: Challenging Wolff's tension/compression interpretation. J Bone Miner Res 14(Suppl 1):S441.
Skerry TM, Lanyon LE. 1995. Interruption of disuse by short duration walking exercise does not prevent bone loss in the sheep calcaneus. Bone 16:269–274.
Skerry TM, Suswillo R, El Hay AJ, Ali NN, Dodds RA, Lanyon LE. 1990. Load-induced proteoglycan orientation in bone tissue in vivo and in vitro. Calcif Tissue Int 46:318–326.
Snow CM. 1996. Exercise and bone mass in young and premenopausal women. Bone, I8(Suppl 1):51S–55S
Su, S. 1998. Microstructure and mineral content correlations to strain parameters in cortical bone of the artiodactyl calcaneus. Masters thesis, University of Utah, Salt Lake City, UT, 64 pp.
Su S, Skedros JG, Bloebaum RD, Bachus KN. 1999. Loading conditions and cortical construction of an artiodactyl calcaneus. J Exp Biol 202:3239–3254.
Takano Y, Turner CH, Owan I, Martin RB, Lau ST, Forwood MR, Burr DB. 1999. Elastic anisotropy and collagen orientation of osteonal bone are dependent upon the mechanical strain distribution. J Orthop Res 17:59–66.
Taylor D. 1997. Bone maintenance and remodeling: a control system based on fatigue damage. J Orthop Res 15:601–606.
Thomas T, Vico L, Skerry TM, Caulin F, Lanyon LE, Alexandre C, Lafage MH. 1996. Architectural modifications and cellular response during disuse-related bone loss in calcaneus of the sheep. J Appl Physiol 80:198–202.
Thompson DW. 1942. On growth and form. New York: Dover.
Turner CH. 1991. Homeostatic control of bone structure: an application of feedback theory. Bone 12:203–217.
Turner CH. 1998. Three rules for bone adaptation to mechanical stimuli. Bone 23:399–407.
Turner CH. 1999. Toward a mathematical description of bone biology: The principle of cellular accommodation. Calcif Tissue Int 65:466–471.
Turner CH. 2000. Letter to the editor. Reply. Calcif Tissue Int 67: 184–187.
Turner CH, Takano, Y, Owan I. 1995. Aging changes mechanical loading thresholds for bone formation in rats. J Bone and Miner Res 10:1544–1549.
van der Meulen MCH, Ashford MW Jr, Kiratli BJ, Bachrach LK, Carter DR. 1996. Determinants of femoral geometry and structure during adolescent growth. J Orthop Res 14:22–29.
van Reitbergen B, Huiskes R, Weinans H, Sumner DR, Turner TM, Galante JO. 1993. The mechanism of bone remodeling and resorption around press-fitted THA stems. J Biomech 26:369–382.
Weinans H, Huiskes R, Grootenboer HJ. 1992. Effects of material properties of femoral hip components on bone remodeling. J Orthop Res 10:845–853.
Weinans H, Huiskes R, Grootenboer HJ. 1994. Effects of fit and bonding characteristics of femoral stems on adaptive bone remodeling. J Biomech Eng 116:393–400.
Weinbaum S, Cowin SC, Zeng Y. 1994. A model for the excitation of osteocytes by mechanical loading-induced bone fluid shear stresses. J Biomech 27:339–360..
Whalen RT, Carter DR, Steele CR. 1988. Influence of physical activity on the regulation of bone density. J Biomech 21:825–837.
Wolff J. 1892. Das Gesetz der Transformation der Knochen. Berlin: A. Hirschwald.
Woo S L-Y, Keui SC, Amiel D, Gomez MA, Hayes WC, White FC, Akeson WH. 1981. The effect of prolonged physical training on the properties of long bone: a study of Wolff's law. J Bone Joint Surg 63-A:780–787.

APPENDIX

Terminology: The Mechanostat Paradigm and Bone Adaptation

Frost's Mechanostat hypothesis and its corollaries represent an extensive formulation of Wolff's law of mechan-

ically induced bone adaptation (Burr, 1992; Frost, 1990a,b, 1997, Frost, 2000b; Wolff, 1892;). The term "Mechanostat paradigm" is used herein to refer to the general Mechanostat hypothesis and its auxiliary hypotheses and corollaries. The Mechanostat "paradigm" is one aspect of what Frost calls the "Utah paradigm" of skeletal physiology (H.M. Frost, personal communication). The Mechanostat paradigm includes the "three-way rule" of bone modeling, the "four-way rule" of bone remodeling, and the Flexion Neutralization Theory.

The three-way rule of bone modeling includes an *endload operator*, a *local strain operator*, and a *cortical drift operator*. The endload operator, alpha, equals −1 for frequent compression or zero endloads and +1 for frequent tension endloads. The local strain operator, beta, equals −1 for frequent compression or concave-tending bending strains equal to or exceeding the minimum effective strain (MES) for modeling; +1 for frequent tension or convex-tending bending strains equal to or exceeding the MES; and zero where strains stay below the MES. The drift operator, gamma, can equal 1 for a resorption drift, zero for no drift, and +1 for a formation drift (Frost 1990a, p 405–406). Frost provides an arithmetic expression that incorporates these three operators and allows predictions of basic modeling activities (resorption, formation, or quiescence).

The four-way rule of bone remodeling includes a *mechanical usage function*, the *BMU (basic multicellular unit) activation function*, and the *two BMU fractions* that signify the amount of bone resorbed and formed by a BMU (Frost, 1990b). Frost describes arithmetic expressions that incorporate these four functions. These expressions allow predictions of some changes in bone formation, resorption, balance, turnover, and remodeling space that depend on how BMU remodeling responds to the "vigor" of mechanical usage.

More detailed descriptions of the three-way and four-way rules and other aspects of the Mechanostat paradigm and the comprehensive Utah paradigm can be found in Martin and Burr (1989) and Frost (1990a,b, 1996, 1997, 1998b).

The general Mechanostat hypothesis is primarily based on the idea that mechanically induced bone strains have an important role in governing *threshold*-related activation and control of bone modeling and remodeling processes. Other investigators have also suggested rules of bone adaptation that generally consider that bone homeostasis is maintained over some range of routine daily stress/strain stimuli, while departures above or below certain stimulus thresholds ("setpoints") initiate formation or resorption of bone, respectively (Beaupre et al., 1990a,b; Burr, 1992; Carter, 1982; Carter et al., 1987, 1996; Cowin, 1984; Fisher et al., 1995; Huiskes et al., 1992; Jacobs et al., 1995; Levenston et al., 1993; Rubin and Lanyon, 1987; Thompson, 1942; Turner, 1991, 1998; Whalen et al., 1988; van Rietbergen et al., 1993; Weinans et al., 1992, 1994).

Adaptation, Modeling, and Remodeling

Since the publication of Wolff's treatise in 1892, *The Law of the Transformation of Bone*, there has been an evolution in the connotations of the rubrics "adaptation," "modeling," and "remodeling," in bone (Currey, 1984; Frost, 1987; Hecht, 1992; Martin and Burr, 1989).

Adaptation. Adaptation in cortical bone commonly refers to either: 1.) changes in bone structure and/or material organization in response to loading conditions outside a normal physiologic stress/strain range, distribution, and/or duration (e.g., Biewener and Bertram, 1994; Currey, 1984; Lanyon et al., 1979; Martin and Burr, 1989; Schaffler et al., 1985; Woo et al., 1981), or 2.) the presence of regional differences in structural and/or material organization that are strongly influenced by normal epigenetic stimuli occurring during *normal* development within or between bones (e.g., Bertram and Swartz, 1991; Currey, 1984; Martin and Burr, 1989; Riggs et al., 1993a,b; Skedros et al., 1994a,b). In the present investigation, "adaptations" are considered to be mechanically relevant regional variations and temporal changes in cortical bone structural and material organization that are produced by the modeling and remodeling processes during *normal* skeletal development.

Modeling. Adaptations resulting from modeling activities include the accretion and/or resorption of secondary or nonsecondary bone (e.g., circumferential lamellae, and trabecular bone in some cases) on periosteal or endosteal surfaces. They are detected as changes and/or differences in a bone's curvature, cross-sectional shape, and/or regional cortical thickness. Consequently, modeling is a concept describing a combination of non-proximate, though coordinated, resorption and formation drifts whose net result is to change the distribution of bone (Jee et al., 1991). Such drifts are called macro-modeling in cortical bone and mini-modeling in cancellous bone (Frost, 1988a,b, 1989). The generic term "modeling" is used herein to describe growth-related macro-modeling.

Remodeling. Adaptations produced by remodeling activities involve the replacement of intracortical bone; this is achieved through the intracortical activation of basic multicellular units (BMUs), which create secondary osteons (Haversian systems) in cortical bone (Frost, 1986; Jee et al., 1991; Parfitt et al., 1996). Manifestations of remodeling adaptations include regional changes and/or differences in secondary osteon population density (N.On/Ar), fractional area of secondary bone (On.B/Ar), cross-sectional area of individual secondary osteons (On.Ar), and/or porosity. If a bone has increased On.B/Ar, then the bone is more "remodeled." In contrast, "remodeling" connotes an active renewal process (Parfitt et al., 1996). Remodeling rates are the primary determinant of mineralization differences in the bone matrix within the cortices of many bones (Grynpas, 1993; Martin, 1993). A relatively increased remodeling rate in a region of bone is detected in the present investigation as relatively decreased bone matrix mineral content and increased population densities of resorption spaces and newly forming secondary osteons (Skedros et al., 1997).

Additional definitions of Mechanostat terminology can be found in the Discussion.